Atmos. Chem. Phys. Discuss., 14, 16529–16589, 2014
www.atmos-chem-phys-discuss.net/14/16529/2014/
doi:10.5194/acpd-14-16529-2014

Atmospheric Chemistry and Physics Discussions

Relations between erythemal UV dose, global solar radiation, total ozone column and aerosol optical depth at Uccle, Belgium

V. De Bock, H. De Backer, R. Van Malderen, A. Mangold, and A. Delcloo

Royal Meteorological Institute of Belgium, Ringlaan 3, 1180 Brussels, Belgium

Received: 25 April 2014 – Accepted: 6 June 2014 – Published: 24 June 2014

Correspondence to: V. De Bock (veerle.debock@meteo.be)

Published by Copernicus Publications on behalf of the European Geosciences Union.

Abstract

At Uccle, a long time series (1991–2013) of simultaneous measurements of erythemal ultraviolet (UV) dose, global solar radiation, total ozone column (TOC) and Aerosol Optical Depth (AOD) (at 320.1 nm) is available which allows for an extensive study of the changes in the variables over time. A change-point analysis, which determines whether there is a significant change in the mean of the time series, is applied to the monthly anomalies time series of the variables. Only for erythemal UV dose and TOC, a significant change point (without any known instrumental cause) was present in the time series around February 1998 and March 1998 respectively. The change point in TOC corresponds with results found in literature, where the change in ozone levels (around 1997) is attributed to the recovery of ozone. Linear trends were determined for the different (monthly anomalies) time series. Erythemal UV dose, global solar radiation and TOC all increase with respectively 7, 4 and 3 % per decade. AOD shows an (insignificant) negative trend of −8 % per decade. These trends agree with results found in literature for sites with comparable latitudes. A multiple linear regression (MLR) analysis is applied to the data in order to study the influence of global solar radiation, TOC and AOD on the erythemal UV dose. Together these parameters are able to explain 94 % of the variation in erythemal UV dose. Most of the variation (56 %) in erythemal UV dose is explained by global solar radiation. The regression model performs well with a slight tendency to underestimate the measured erythemal UV doses and with a Mean Absolute Bias Error (MABE) of 18 %. However, in winter, negative erythemal UV dose values are modeled. Applying the MLR to the individual seasons solves this issue. The seasonal models have an adjusted R^2 value higher than 0.8 and the correlation between modeled and measured erythemal UV dose values is higher than 0.9 for each season. The summer model gives the best performance, with an absolute mean error of only 6 %. Again, global solar radiation is the factor that contributes the most to the variation in erythemal UV dose, so there is no doubt about the necessity to include this factor in the regression models. A large part of the influence of AOD is already

ACPD
14, 16529–16589, 2014

represented by the global solar radiation parameter. Therefore the individual contribution of AOD to erythemal UV dose is so low. For this reason, it seems unnecessary to include AOD in the MLR analysis. Including TOC however, is justified as the adjusted R^2 increases and the MABE of the model decreases compared to a model where only global solar radiation is used as explanatory variable.

1 Introduction

The discovery of the Antarctic Ozone hole in the mid-1980s triggered an increased scientific interest in the state of stratospheric ozone levels on a global scale (Garane et al., 2006). The ozone depletion not only occurred above the Antarctic, but there is strong evidence that stratospheric ozone also diminished above mid-latitudes (Bartlett and Webb, 2000; Kaurola et al., 2000; Smedley et al., 2012). While ozone depletion continued in the 2000s over the polar regions, it has leveled off at mid-latitudes, although ozone amounts still remain lower compared to the amounts in the 1970s (Garane et al., 2006). Stratospheric ozone is expected to recover in response to the ban on ozone depleting substances agreed by the Montréal Protocol in 1987 (WMO, 2006; Fitzka et al., 2012). However, it is difficult to predict future changes in ozone as the predictions suffer from uncertainties caused by the general climate change, numerical errors of simulation models and by human behaviour which is not well controllable in several parts of the world. The decline in stratospheric ozone has shifted the focus of the scientific community and the general public towards the variability of surface UV irradiance (Krzyścin et al., 2011). If all other factors influencing UV irradiance remain stable, reductions in stratospheric ozone would lead to an increase in UV irradiance at the ground, particularly at wavelengths below 320 nm (Garane et al., 2006). Increases of UV irradiance in response to the ozone decline have already been reported for different sites during the 1990s (Garane et al., 2006 and references therein).

The possible increase in UV irradiance raises concern because of its adverse health and environmental effects. Overexposure can lead to the development of skin cancers,

ACPD
14, 16529–16589, 2014

cataract, skin aging and the suppression of the immune system (Rieder et al., 2008; Cordero et al., 2009). UV irradiance also has adverse effects on terrestrial plants (Tevini and Teramura, 1989; Cordero et al., 2009) and on other elements of the biosphere (Diffey, 1991). On the other hand, UV radiaton does enable the production of vitamin D in the skin, which is positively linked to health effects as it supports bone health and may decrease the risk of several internal cancers (Bernhard, 2011). It is important to assess the changes in UV irradiance over prolonged periods of time. Not only do adverse health and environmental effects often relate to long term exposure (from years to a lifetime), also the time scales of the atmospheric processes that are involved (e.g. ozone depletion and recovery) are beyond decades (Chubarova, 2008; den Outer et al., 2010).

In principle, long term trends in UV irradiance can either be inferred from direct measurements (from ground or space) or reconstructed based on proxy data such as total ozone and sunshine duration (Bernhard, 2011). Different sorts of reconstruction models have been used in several studies. They all use various kinds of statistical or model approaches and different meteorological or irradiance datasets (Chubarova, 2008; Rieder et al., 2010; den Outer et al., 2010; Bais et al., 2011). Techniques are either based on modeling of clear sky UV irradiance or on empirical relationships between surface UV irradiance and the factors influencing the penetration of UV irradiance through the atmosphere (Kaurola et al., 2000; Trepte and Winkler, 2004). In addition to the reconstruction studies, changes in surface UV irradiance have also been studied using ground based measurements at different locations (e.g. den Outer et al., 2000; Sasaki et al., 2002; Bernhard et al., 2006; Fitzka et al., 2012; Zerefos et al., 2012) or even in combination with satellite retrievals (Herman et al., 1996; Matthijsen et al., 2000; Kalliskota et al., 2000; Ziemke et al., 2000; Zerefos et al., 2001; Fioletov et al., 2004; Williams et al., 2004). Some studies combine both models and observations to investigate possible UV irradiance changes (e.g. Kaurola et al., 2000).

Not only stratospheric ozone influences the intensity of UV irradiance reaching the surface of the Earth. Long term changes in solar elevation, tropospheric ozone, clouds,

ACPD
14, 16529–16589, 2014

Rayleigh scattering on air molecules, surface albedo, aerosols, absorption by trace gases and changes in the distance between the Sun and the Earth can lead to trends in UV irradiance (Bernhard, 2011). Some studies show that increased amounts of aerosols and trace gases from industrial emissions, which absorb UV irradiance in the troposphere, could even compensate for the UV effects caused by the stratospheric ozone decline (Krzýscin et al., 2011; Fitzka et al., 2012). Clouds induce more variability in surface UV irradiance than any other geophysical factor, but their effects depend very much on local conditions (Krzýscin et al., 2011). Surface albedo is determined mostly by snow amount and snow depth (Rieder et al., 2010) and plays a significant role at high altitude and high latitude sites, where UV irradiance can be strongly enhanced due to multiple occurrences of scattering and reflection between snow covered ground and the atmosphere (Fitzka et al., 2012). Several studies have been conducted to quantify the effects of the above mentioned variables on the amount of UV irradiance reaching the ground and many of them have done so by constructing empirical models with UV irradiance (or a related quantity) as a dependent variable (Díaz et al., 2000; Fioletov et al., 2001; de la Casinière et al., 2002; Foyo-Moreno et al., 2007; Antón et al., 2009; De Backer, 2009; Huang et al., 2011; Krishna Prasad et al., 2011; El Shazly et al., 2012).

At Uccle, simultaneous measurements of erythemal UV dose, global solar radiation, total ozone column and AOD at 320.1 nm are available for a long time period of 23 years (1991–2013). The time series is long enough to allow for reliable determination of significant changes (a minimum of 15 years is required as shown in Weatherhead et al., 1998 and Glandorf et al., 2005). The availability of the simultaneous time series allows an extensive analysis in which three analysis techniques (change-point analysis, linear trend analysis and multiple linear regression analysis) will be combined in order to increase our insights in the relations between the variables. The monthly anomalies time series will be the subject of change-point analysis where the homogeneity of the time series will be investigated. Next, a linear trend analysis will be applied to the monthly anomalies of the time series (both on a daily and seasonal time scale) and the results

ACPD
14, 16529–16589, 2014

will be compared with results found in literature. Monthly anomalies are used to reduce the influence of the seasonal cycle on the analysis and are calculated by subtracting the long term monthly mean from the individual monthly means. Finally, the multiple linear regression technique (with daily erythemal UV doses as dependent variable and daily values of global solar radiation, total ozone column and AOD at 320.1 nm as explanatory variables) will allow us to study the influence of the explanatory variables on the dependent variable on a daily and seasonal basis.

2 Data

In this study, the (all sky) erythemal UV dose, (all sky) global solar radiation, total ozone column and (clear sky) AOD at 320.1 nm are investigated over a time period of 23 years (1991–2013). These measurements are performed at Uccle, Belgium (50°48' N, 4°21' E, 100 m a.s.l.), a residential suburb of Brussels located about 100 km from the North Sea shore.

2.1 Daily erythemal UV dose

In 1989, the Brewer spectrophotometer instrument#016 (single monochromator) was equipped with a UV-B monitor (De Backer, 2009). This is an optical assembly which enables the Brewer to measure UV-B irradiance using a thin disc of Teflon as a transmitting diffuser (SCI TEC Brewer#016 manual, 1988). The Brewer measures the horizontal spectral UV irradiance with a spectral resolution of approximately 0.55 nm, full width at half maximum. The instrument performs UV scans from 290 to 325 nm with 0.5 nm wavelength steps (Fioletov et al., 2002). The erythemal irradiances are calculated using the erythemal action spectrum as determined by the Commission Internationale de l'Eclairage and are integrated to daily erythemal doses (De Backer, 2009). For wavelenghts above 325 nm (for which Brewer#016 does not provide data), the intensities are extrapolated using a theoretical spectrum weighted by the intensity at 325 nm. This

ACPD
14, 16529–16589, 2014

is justified by the fact that, at those wavelengts, the UV intensity is no longer strongly dependent on ozone and the erythemal weighting function is low. For the calculation of the daily sum, a linear interpolation between the different measurement points is performed. When there is an interruption between the measurements (between sunrise and sunset) of 2 h or more, the calculated daily sum is rejected. The data (in $J\,m^{-2}$) are available on a regular base since 1991. The instrument is calibrated with 50 W lamps on a monthly basis and with 1000 W lamps during intercomparisons in 1994, 2003, 2006, 2008, 2010 and 2012. The instrument was also compared with the travelling QUASUME unit in 2004 (Gröbner et al., 2004).

2.2 Global solar radiation

The global solar radiation is a measure of the rate of total incoming solar energy (both direct and diffuse) on a horizontal plane at the surface of the Earth (Journée and Bertrand, 2010). The measurements at Uccle are performed by CM11 pyranometers (Kipp&Zonen; http://www.kippzonen.com). For this study, the daily values in $J\,m^{-2}$ (derived from 10 min and 30 min data) are used. The data are quality controlled in two steps: first a preliminary fully automatic quality control is performed prior to the systematic manual check of the data (Journée and Bertrand, 2010). In May 1996, we switched to a new system and in 2005 half of the instruments were replaced. Corrections to the measurements have been done in 2000, 2001, 2004, 2005, 2007 and 2012. (For the period before 1996, no information is available concerning possible calibrations of the instrument.)

2.3 Total ozone column

Total ozone column values (in DU) are available from Brewer#016 direct sun measurements. The instrument records raw photon counts of the photomultiplier at 5 wavelengths (306.3, 310.1, 313.5, 316.8 and 320.1 nm) using a blocking slit mask, which opens successively one of the five exit slits. The five exit slits are scanned twice within

ACPD
14, 16529–16589, 2014

1.6 s and this is repeated 20 times. The whole procedure is repeated five times for a total of about three minutes. The total ozone column is obtained from a combination of measurements at 310.1, 313.5, 316.8 and 320.1 nm, weighted with a predefined set of constants chosen to minimize the influence of SO_2 and linearly varying absorption features from e.g. clouds or aerosols (Gröbner and Meleti, 2004). Brewer#016 was calibrated relative to the Dobson instrument in 1984 (De Backer and De Muer, 1991) and regularly recalibrated against the travelling standard Brewer instrument #017 in 1994, 2003, 2006, 2008, 2010 and 2012. The stability is also continuously checked against the co-located instruments Dobson#40 (from 1991 until May 2009) and Brewer#178 (since 2001).

2.4 Aerosol Optical Depth

Cheymol and De Backer (2003) developed a method that enables the retrieval of AOD values (at 306.3, 310.1, 313.5, 316.8 and 320.1 nm) using the Direct Sun (DS) measurements of the Brewer instrument. It is also possible to retrieve AOD values at 340 nm using Sun Scan (SS) measurements of the Brewer instrument (De Bock et al., 2010). Together with the AOD retrieval method, De Bock et al. (2010) developed a cloud screening procedure to select the clear sky AOD values. However, this screening method did not perform well. Hence an improved cloud screening method (described in Sect. 3.1) has been developed and has been applied to AOD values retrieved from DS and SS measurements. For this study only the cloud screened AOD values at 320.1 nm, retrieved from the DS measurements of the single monochromator Brewer#016, will be used.

ACPD
14, 16529–16589, 2014

3 Method

3.1 Improved AOD cloud screening method

The initial cloud screening algorithm, as described in De Bock et al., 2010, consisted of three steps. First, all AOD values larger than 2 were removed. Then, it was verified whether there was a DS observation within five minutes of each individual AOD measurement. Finally, the measured irradiances (photon counts) were plotted for days with AOD measurement(s) larger than 1.5. If the graph showed clear signs of cloud perturbation, the measurement was removed. The first two steps of this cloud screening were done automatically, whereas the last step had to be done manually. Analysis of the cloud screened data indicated that the performance of this screening technique was not optimal. Therefore it was decided to develop an improved cloud screening method.

This new cloud screening method makes use of sunshine duration data (from 4 pyrheliometers at Uccle) and is also based on the assumption that the variability of the AOD in the course of one day is either lower than 10 % or lower than 0.08 AOD units (which is the maximum uncertainty of the AOD retrieval algorithm). Figure 1 gives a schematic overview of the improved cloud screening technique. First it is determined whether the individual AOD measurements were taken within a 10 min interval of continuous sunshine. The measurements for which this is not the case are removed, after which more than 2 individual measurements per day must remain in order to continue. For each day, we then determine the maximum deviation to the median value. If this value is less than 0.08, we accept all measurements for that day. However, if the maximum deviation exceeds 0.08, the relative standard deviation for that day is calculated. In case this value is less than 10 % (which would guarantee a given stability within the diurnal pattern of AOD), all the AOD values for that day are accepted. In the other case, the AOD measurement with the largest contribution to the standard deviation is removed (as this measurement is most likely influenced by clouds). The median value will then be recomputed and the previous steps are repeated. Days with 2 or less

ACPD
14, 16529–16589, 2014

individual AOD measurements are excluded from the results, since it does not make sense to calculate the deviation to the median and the standard deviation.

The cloud-screened AODs (both from DS and SS Brewer measurements) were compared to quasi-simultaneous and co-located Cimel level 2.0 quality assured values (with a maximum time difference of 3 min). The Cimel sunphotometer, which belongs to BISA (Belgium Institute of Space Aeronomy), is located at approximately 100 m from the Brewer instrument. It is an automatic sun-sky scanning filter radiometer allowing the measurements of the direct solar irradiance at wavelengths 340, 380, 440, 500, 670, 870, 940 and 1020 nm. These solar extinction measurements are used to compute aerosol optical depth at each wavelength except for the 940 nm channel, which is used to retrieve total atmospheric column precipitable water in centimeters. The instrument is part of the AERONET network (http://aeronet.gsfc.nasa.gov/; Holben et al., 2001). The accuracy of the AERONET AOD measurements at 340 nm is 0.02 (Eck et al., 1999). For the period of comparison (2006–2013), the correlation coefficient, slope and intercept of the regression lines have been calculated and the values are presented in Table 1. The results of the comparison show that the cloud screened Brewer AOD values agree very well with the Cimel data.

The advantages of the improved cloud screening method are the removal of the arbitrary maximum level of AOD values and the fact that it runs completely automatic (whereas the old one needed manual verification afterwards). This method has now been applied not only to the AOD retrieval using SS measurements at 340 nm, but also to the method using DS measurements.

3.2 Data analysis methods

Since most statistical analysis tests, such as linear regression and change-point tests, rely on independent and identically distributed time series (e.g. Van Malderen and De Backer, 2010 and references therein), most data used in this study are in their anomaly form. Monthly anomalies are used to reduce the influence of the seasonal cycle on the analysis and are calculated by subtracting the long term monthly mean from the

ACPD
14, 16529–16589, 2014

individual monthly means. Monthly means are only calculated for months with at least 10 individual daily values. For the multiple linear regression analysis, daily values will be used instead of anomaly values.

3.2.1 Change-point analysis

Change points are times of discontinuity in a time series (Reeves et al., 2007) and can either arise naturally or as a result of errors or changes in instrumentation, recording practices, data transmission, processing, etc. (Lanzante, 1996). A change point is said to occur at some point in the sequence if all the values up to and including it share a common statistical distribution and all those after the point share another. The most common change-point problem involves a change in the mean of the time series (Lanzante, 1996). There are different tests that can be used to detect a change point in a time series. In this study we use the combination of three tests: the non-parametric Pettitt–Mann–Whitney (PMW) test (based on the ranks of the values in the sequence), the Mann–Whitney–Wilcoxon (MWW) test (a rank sum test) and the Cumulative Sum Technique (CST). The details of these tests are described in Hoppy and Kiely (1999). The change points discussed further in this study are detected by all three tests (except when mentioned otherwise) and only the change points that exceeded the 90 % confidence level were retained. The change points are determined for the monthly anomalies time series of erythemal UV doses, global solar radiation, TOC and AOD at 320.1 nm.

3.2.2 Linear trend analysis

Linear trends are calculated for the monthly anomalies of erythemal UV dose, global solar radiation, TOC and AOD at 320.1 nm. To determine the significance of the linear trends, the method described in Santer et al. (2000) is used. The least squares linear regression estimate of the trend in $x(t)$, b, minimizes the squared differences between

ACPD
14, 16529–16589, 2014

$x(t)$ and the regression line $\hat{x}(t)$

$$\hat{x}(t) = a + b(t); \quad t = 1, \ldots, n_t \tag{1}$$

Whether a trend in $x(t)$ is significantly different from zero is tested by computing the ratio between the estimated trend (b) and its standard error (s_b)

$$t_b = \frac{b}{s_b} \tag{2}$$

Under the assumption that t_b is distributed as Student's t, the calculated t ratio is then compared with a critical t value, t_{crit}, for a stipulated significance level α and $n_t - 2$ degrees of freedom (Santer et al., 2000).

However, if the regression residuals are autocorrelated, the results of the regression analysis will be too liberal and the original approach must be modified. The method proposed in Santer et al. (2000) involves the use of an effective sample size n_e in the computation of the adjusted standard error and calculated t value, but also in the indexing of the critical t value. To test for autocorrelation in the residuals of a time series, the Durbin–Watson test is used (Durbin and Watson, 1971).

The above described linear trend analysis is also applied to the monthly anomalies of the extreme values (minima and maxima) of the variables. The extreme values are calculated by determining the lowest and highest measured value for each month. These trends will be studied together with the relative frequency distribution of the daily mean values. This distribution is determined by using the minimum and maximum values of the entire study period as boundaries and by dividing the range between the boundaries into a certain amount of bins of equal size. The daily values are distributed over the different bins and the relative frequency (in %) is calculated. This will be done for 2 different time periods: 1991–2002 and 2003–2013. Also, the medians for these periods are calculated. In this way, it is possible to investigate whether there is a shift in the frequency distribution of the variables from the first period to the second one. (The results of the analysis of the frequency distribution will only be presented in case they show a significant shift in the data).

ACPD
14, 16529–16589, 2014

3.2.3 Multiple linear regression analysis

The goal of a Multiple Linear Regression (MLR) analysis is to determine the values of parameters for a linear function that cause this function to best describe a set of provided observations (Krishna Prasad et al., 2011). In this study, the MLR technique is used to explore whether there is a significant relationship between the erythemal UV dose and three explanatory variables (global solar radiation, TOC and AOD) both on a daily and seasonal scale. We use a linear model where the coefficients are determined with the least squares method:

$$S_{ery} = a \times S_g + b \times Q_{O_3} + c \times \tau_{aer} + d + \epsilon \quad (3)$$

with

- S_{ery}: erythemal UV dose (in J m^{-2})
- S_g: global radiation (in J m^{-2})
- Q_{O_3}: total ozone column (in DU)
- τ_{aer}: Aerosol Optical Depth at 320.1 nm
- a, b, c: regression coefficients
- d: constant term
- ϵ: error term.

The model will be developed based on data from 1991 to 2008. The data from 2009 to 2013 will be used for validation of the model. The performance of the model and its parameters will be evaluated through different statistical parameters. The adjusted R^2 value is the measure for the fraction of variation in UV explained by the regression, accounting for both the sample size and the number of explanatory variables. Compared to the R^2 value, the adjusted R^2 value will only increase if a new variable has

ACPD
14, 16529–16589, 2014

additional explanatory power. It is possible to test the null hypothesis that a regression coefficient is equal to zero (which would mean that the variable associated with this regression coefficient does not contribute to explaining the variation in UV) by looking at the p value. If we want to test whether a regression coefficient differs significantly from zero at the 5 % level, the p value should be less than or equal to 0.05. The influence of the variation in the three parameters on the variation of S_{ery} is determined by multiplying the standard deviation of each parameter with its corresponding regression coefficient and dividing this by the average S_{ery} value.

The Mean Bias Error (MBE) and the Mean Absolute Bias Error (MABE) are also calculated in order to evaluate the performance of the regression model. The MBE (given in %) provides the mean relative difference between modeled and measured values (Antón et al., 2009):

$$\mathrm{MBE} = 100 \times \frac{1}{N} \sum_{i=1}^{N} \frac{S_{\mathrm{ery}_i}^{\mathrm{modeled}} - S_{\mathrm{ery}_i}^{\mathrm{measured}}}{S_{\mathrm{ery}_i}^{\mathrm{measured}}} \tag{4}$$

The MABE (given in %) reports on the absolute value of the individual differences between modeled and measured data (Antón et al., 2009):

$$\mathrm{MABE} = 100 \times \frac{1}{N} \sum_{i=1}^{N} \frac{\left|S_{\mathrm{ery}_i}^{\mathrm{modeled}} - S_{\mathrm{ery}_i}^{\mathrm{measured}}\right|}{S_{\mathrm{ery}_i}^{\mathrm{measured}}} \tag{5}$$

ACPD
14, 16529–16589, 2014

4 Results and discussion

4.1 Change-point analysis

4.1.1 Erythemal UV dose

According to the three tests (PMW, MWW and CST) of the change-point analysis, there is a significant shift in the mean of the monthly anomalies of erythemal UV dose which occurs around January 2003. The change point is located suspiciously close to the middle of the time series though. To remove the influence of the presence of one general increasing trend (which would lead to the discovery of a change point in the middle of the time series), the time series was detrended (= original time series – general trend). The change point in the detrended time series is located around February 1998 (Fig. 2). Since no calibration of the Brewer instrument took place around that period, it seems that the change point is not caused by known instrumental changes but rather by natural/environmental changes.

4.1.2 Global solar radiation

A significant change point was detected (only by the PMW test) around January 2003 in the time series of global solar radiation. Similar to the erythemal UV dose time series, there is one general trend present, which explains the detection of a change point near the middle of the time series. Thus, it was again decided to look at the detrended time series of global radiation. However, the detected change point around January 2006 (only by the PMW test) was not significant at the 90 % significance level.

4.1.3 Total ozone column

All three tests confirmed the presence of a significant change point around March 1998 in the time series of monthly anomalies of TOC, where the mean before the change point is clearly lower than the one after the change point (Fig. 3). As there is clearly

ACPD
14, 16529–16589, 2014

more than one general trend within the entire time series, there is no need for detrending in this case. No ozone calibrations were performed around 1998, so the change point has no known instrumental cause.

4.1.4 AOD at 320.1 nm

According to the change-point analysis, no significant change was found in the mean of the monthly anomalies of AOD.

4.1.5 Overview and explanations

The change points in the time series of erythemal UV dose and TOC occur around the same time period (February/March 1998). Since we were able to rule out known instrumental causes for the detected change points in both time series, we can assume that they have some natural/environmental cause and are related to each other.

The change point in the TOC time series corresponds with results found in literature. Recent studies have shown that for other stations, the ozone recovery started around 1997 (Steinbrecht et al., 2006; Reinsel et al., 2005). Ozone levels seem to follow the change in chlorine concentrations resulting from the regulations of the Montréal Protocol in 1987. When ozone starts to increase, it is expected to have some implications on the UV irradiance as ozone is a strong absorber of UV irradiance in the stratosphere (Wenny et al., 2001). An increase in ozone would normally lead to a decrease in UV irradiance, which is not what was observed at Uccle where the UV irradiance levels continue to increase after 1998. Before 1998, the (insignificant) trends in the time series of TOC and erythemal UV dose are opposite, which is what would be expected. However after 1998, both the (insignificant) TOC and erythemal UV dose trend are positive. So the behavior of TOC can only partly explain the changes observed in the UV irradiance time series and other parameters (such as aerosols and cloudiness) might play an important role.

ACPD
14, 16529–16589, 2014

4.2 Linear trend analysis

4.2.1 Erythemal UV dose

A significant positive trend (at the 99 % significance level) can be detected in the time series of monthly anomalies of erythemal UV doses (Fig. 4). These values increase with 7 % (±2 %) per decade. The seasonal trends are presented in Table 2. In spring (March, April and May), summer (June, July and August) and autumn (September, October and November), the erythemal UV dose increases significantly, whereas in winter (December, January and February), the trend is negative. The increase in erythemal UV dose is the largest in spring.

A significant positive trend has been found in the monthly anomalies of both the minimum and maximum values of erythemal UV dose. The minimum values show an increase of +10 % (±4 %) per decade and the maximum values increased by 7 % (±1 %) per decade (respectively at the 95 and 99 % level). The increase in the median value from 825 J m^{-2} (1991–2002) to 987 J m^{-2} (2003–2013), shows that higher erythemal UV dose values are more frequent in the last period.

4.2.2 Global solar radiation

The values of the global solar radiation show an increase of 4 % (±1 %) per decade at the 99 % significance level, which corresponds to an absolute change of +0.5 (±0.2) W m^{-2} year^{-1} for the observed time period (Fig. 4). On a seasonal scale, spring and autumn exhibit a significant positive trend (Table 3). The seasonal trends of global solar radiation, although not significant in summer and winter, have the same sign as the seasonal erythemal UV dose trends. The trends of global solar radiation are smaller than the UV trends, both on an annual and seasonal scale.

There is a clear difference between the trends of the monthly anomalies of minimum and maximum values of global solar radiation. Both trends are positive, but the increase in the minimum values (+12 % (±5 %) per decade at 99 % significance level) is much

ACPD
14, 16529–16589, 2014

larger than the one in the maximum values (+3.2 % (±0.7 %) per decade at 99 % significance level). Study of the median values reveals the presence of an increase from 7880 kJ m^{-2} (1991–2002) to 8902 kJ m^{-2} (2003–2013). As the global radiation data are all sky data, it is obvious that the minimum values are the ones that are influenced by clouds. If the minimum values increase in time, this could mean that the cloud properties (such as cloud optical depth) changed over the past 23 years. However, this is difficult to prove without direct information or measurements on cloud amount and/or properties.

4.2.3 Total ozone column

The monthly anomalies of TOC show a positive trend of 2.6 % (±0.4 %) per decade (significant at 99 %) (Fig. 4). Significant positive trends occur in spring and summer (Table 4), with the trend in spring being the largest one. As opposed to the seasonal trends of erythemal UV dose and global radiation, the ones for TOC are positive for each season. We would expect an increase in TOC over the past 23 years to be accompanied by a decrease in erythemal UV dose, which is not the case for the Uccle time series. This indicates that other variables might contribute to the change in erythemal UV dose and the contribution of TOC might be washed out by the influence of these other variables.

Both the minimum and maximum TOC values increased significantly (99 % level) at the same rate (+3.0 % (±0.6 %) per decade for the minimum values and +3.1 % (±0.6 %) per decade for the maximum values) over the past 23 years. A clear shift can be seen in the frequency distribution (Fig. 5) of the daily TOC values. During the second period (2003–2013), higher values are more frequent than during the previous period (1991–2002), which is supported by the increase in median values from 319.3 DU (1991–2002) to 327.9 DU (2003–2013). The entire curve of the frequency distribution is shifted, which means that the minimum values of the distribution have also increased between the two decades. After a period with lower TOC values in the 1990s, it seems that ozone has been recovering over the past 10 years.

ACPD
14, 16529–16589, 2014

4.2.4 AOD at 320.1 nm

While the overall trends of erythemal UV dose, global solar radiation and TOC are all positive, the AOD values at 320.1 nm show a negative trend of −8 % (±5 %) per decade. This trend however is not significant (Fig. 4). The seasonal trends (Table 5) show that the summer and autumn trends are significantly negative, with the largest trend being observed during autumn. Due to a lack of sufficient clear sky data, it was not possible to determine the winter trend for AOD.

There are no significant changes in the minimum and maximum AOD values over the 1991–2013 period. From the relative frequency distribution of the daily AOD values (Fig. 6), it can be seen that the frequency of lower AOD values (AOD < 0.4) was higher during the second period (2003–2013). Also the frequency of high AOD values (AOD > 0.7) has decreased towards the second decade. This is in agreement with the overall decrease in AOD over the last 23 years. However, this is not obvious from the median values as they decreased only slightly from 0.38 (1991–2002) to 0.36 (2003–2013).

4.3 Comparison of Uccle trends with other stations

4.3.1 Erythemal UV dose

Long term UV trends for different locations around the world have been the subject of many research articles and it is worth checking the consistency of our results with these studies even though the time periods are never exactly the same as the one studied in this paper (1991–2013). Some trends (observed or modeled/reconstructed) found in literature are presented in Table 6. Looking at these trends, it can be seen that for the stations with comparable latitude to Uccle (45–55° N, stations in blue in Table 6), the trends in UV range from −2.1 to +8.6 % per decade. The increase of 7 % (±2 %) per decade observed at Uccle falls within the range of trends reported in literature. On a more global scale, Zerefos et al. (2012) examined UV irradiance over selected sites in Canada, Europe and Japan between 1990 and 2011. The results (based on

ACPD
14, 16529–16589, 2014

observations and modeling for all stations) showed an increase in UV irradiances of 3.7 % (±0.5 %) and 5.5 % (±0.3 %) per decade at respectively 305 and 325 nm. For Europe, only the trend at 325 nm (3.4 % (±0.4 %) per decade) was significant. The COST 726 action (Litynska et al., 2009; www.cost726.org) calculated trend values for European sites and saw a mean positive trend of 4.5 % (±0.5 %) per decade since 1980 (derived from reconstruction models, based on TOC and measured total solar irradiance).

4.3.2 Global solar radiation

Concerning the global solar radiation, many publications agree on the existence of a solar dimming period between 1970 and 1985 and a subsequent solar brightening period (Norris and Wild, 2007; Solomon et al., 2007; Makowski et al., 2009; Stjern et al., 2009; Wild et al., 2009; Sanchez-Lorenzo and Wild, 2012). Different studies have calculated the trend in global radiation after 1985. The trend in global radiation from GEBA (Global Energy Balance Archive; http://www.iac.ethz.ch/groups/schaer/research/rad_and_hydro_cycle_global/geba) between 1987 and 2002 is equal to +1.4 (±3.4) $W m^{-2}$ per decade according to Norris and Wild (2007). Stjern et al. (2009) found a total change in the mean surface solar radiation trend over 11 stations in Northern Europe of +4.4 % between 1983 and 2003. In the fourth assessment report of the IPCC (Solomon et al., 2007), 421 sites were analyzed and between 1992 and 2002, the change of all sky surface solar radiation was equal to 0.66 $W m^{-2}$ $year^{-1}$. Wild et al. (2009) investigated the global solar radiation from 133 stations (from GEBA/World Radiation Data Centre) belonging to different regions in Europe. All series showed an increase over the entire period, with a pronounced upward tendency since 2000. For the Benelux region, the linear change between 1985 and 2005 is equal to +0.42 $W m^{-2}$ per year, compared to the Pan-European average trend of +0.33 $W m^{-2}$ per year (or +0.24 $W m^{-2}$ if the anomaly of the 2003 heat wave is excluded) (Wild et al., 2009). Our trend at Uccle of +0.5 (±0.2) $W m^{-2}$ $year^{-1}$ (or +4 % per decade) agrees within the error bars with the results from Wild et al. (2009), but seems to be somewhat at the high end range.

ACPD
14, 16529–16589, 2014

4.3.3 Total ozone column

Ozone and its trends have been the subject of scientific research since the discovery of ozone depletion. Many studies agree that ozone has decreased since 1980 to the mid 1990s as a consequence of anthropogenic emissions of Ozone Depletion Substances (ODS). This period of decrease is followed by a period of significant increase (Steinbrecht et al., 2006; Harris et al., 2008; Vigouroux et al., 2008; Krzyścin and Borkowski, 2008; Herman, 2010; Bais et al., 2011). For the period before the mid 1990s, studies report on decreasing ozone values at Brussels (Bojkov et al., 1995 and Zerefos et al., 1997), Reading (Bartlett and Webb, 2000), Lerwick (Smedley et al., 2012), Arosa (Bojkov et al., 1995 and Staehelin et al., 1998), Hohenpeissenberg (Bojkov et al., 1995), Sodankylä (Glandorf et al., 2005) and Thessaloniki (Glandorf et al., 2005) (see Table 7). After the mid-1990s, most studies report on a plateau or a limited increase in ozone. For example, Smedley et al., 2012, found no clear ozone trend in the 1993–2008 period for Reading. Ozone observations from a Brewer instrument at Hoher Sonnblick (by Fitzka et al., 2012), showed a small but significant increase between 1997 and 2011. Similar behavior was reported for Jungfraujoch in Vigouroux et al., 2008. Our result (a trend of +2.6 % per decade) compares well with the trend observed at Hoher Sonnblick (which is the only station with a time period comparable to the one at Uccle). From Fig. 3, it can be seen that a negative trend occurred in the TOC values before 1998 and that this trend was followed by an positive one. However, both trends are not significant at Uccle. It is difficult to unambiguously attribute the ozone trends to changes in ODS because other factors also contribute to ozone variability and trends. These factors are large volcanic eruptions, arctic ozone depletion, long term climate variability, changes in the stratospheric circulation and the eleven year solar cycle (Harris et al., 2008; Vigouroux et al., 2008). According to Rieder et al., 2013, the Equivalent Effective Stratospheric Chlorine and the 11-year solar cycle can be identified as major contributors, but the influence of dynamical features (such as the El Niño Southern Oscillation, North Atlantic

ACPD
14, 16529–16589, 2014

Oscillation and Quasi-Biennial Oscillation) on the ozone variability and trends can not be neglected at a regional level.

4.3.4 AOD at 320.1 nm

Trend analysis studies of long time series of AOD are still very scarce at the moment. Some studies however do report on aerosol trends (Table 8). Mishchenko and Geogdzhayev (2007) observed a significant decrease in AOD from 1991 to 2005 over much of Europe within the GACP (Global Aerosol Climatology Project; http://gacp.giss.nasa.gov/) data. Alpert et al. (2012) studied AOD trends from MODIS (MODerate resolution Imaging Spectroradiometer) and MISR (Multi-angle Imaging SpectroRadiometer) satellite measurements over the 189 largest cities in the world and saw a decrease in AOD over Europe for the 2002–2010 period. The decadal trend observed by de Meij et al. (2012) over Europe between 2000 and 2009 was negative for MODIS (−30 %), MISR (−9 %) and AERONET (−25 %). Zerefos et al. (2012), who investigated the AOD over Europe, Japan and Canada, discovered a general decline in AOD exceeding 10 % year^{-1}. For Europe specifically, the trend of AOD varied between −16.6 % (±6 %) per decade when using the GACP dataset and −42.8 % (±5.7 %) for the MODIS dataset. The (insignificant) trend observed at Uccle (−8 % ± 5 % per decade) lies within the range of trends observed at other European stations. The long term AOD decrease over much of Europe is quite consistent with the supposed reversal from increasing to decreasing anthropogenic sulfur and black carbon emissions owing to the enactment of clean air legislation in many countries (Mishchenko and Geogdzhayev, 2007; Chiaccio et al., 2011; Alpert et al., 2012; de Meij et al., 2012; Hsu et al., 2012; Nabat et al., 2013). This change occurred after 1988–1989, the time period when a maximum was reached in the emissions of sulfate aerosols over Europe (Chiaccio et al., 2011). Many scientists believe that the decadal changes in aerosols have influenced the amount of solar radiation reaching the surface of the Earth and that the decrease in aerosols has played a part in the switch from global dimming to global brightening (which occurred around 1980–1990) (Augustine et al., 2008; Chiaccio et al., 2011). According to Wild

ACPD
14, 16529–16589, 2014

et al. (2009), the reduction of aerosols may have played a role during the 1990s but not after 2000. Decreases in cloudiness or cloud albedo may have enabled the continuation of the increase in surface solar radiation over Europe beyond 2000, despite the stabilization of aerosol concentrations.

4.4 Multiple linear regression analysis

Before applying the Multiple linear regression (MLR) technique, it has to be verified that the explanatory variables (global solar radiation, TOC and AOD) are independent variables. This is done by calculating the correlation coefficients between these parameters. The correlation coefficients between the three variables are low enough (< 0.25) to allow using these variables as independent explanatory variables for the multiple regression analysis. As opposed to the previous analysis methods, the MLR is applied to daily values (instead of monthly anomaly values. For UV and global radiation, the daily sums are used, whereas for ozone and AOD, daily mean values are used.

4.4.1 MLR analysis of daily values using OZON, RAD and AOD

The MLR analysis has been applied to 1246 simultaneous daily values of erythemal UV dose (S_{ery}), global solar radiation (S_g), total ozone (Q_{O_3}) and AOD (τ_{aer}) between 1991 and 2008. (The amount of regression days was highly limited by the available AOD measurements.) The resulting regression equation is:

$$S_{ery} = 690 + 0.000169 \times S_g - 5.01 \times Q_{O_3} + 70.0 \times \tau_{aer} + \epsilon \quad (6)$$

(with S_{ery} in J m^{-2}; S_g in J m^{-2} and Q_{O_3} in DU).

The adjusted R^2 value of the multiple regression is 0.94, which means that S_g, Q_{O_3} and τ_{aer} together explain 94 % of the variation in daily S_{ery}. When looking at the changes in S_{ery} caused by the variation of each of the three parameters (calculated by multiplying the standard deviation of each parameter with its corresponding regression

ACPD
14, 16529–16589, 2014

coefficient and dividing this by the average S_{ery} value), it is clear that S_g (whose variation leads to a change in S_{ery} of 56 %) has the biggest influence on S_{ery}, followed by Q_{O_3} (change in S_{ery} of −9 %) and τ_{aer} (change in S_{ery} of 1 %).

The data from 2009–2013 are used to validate the model (see Fig. 7). The regression equation between the modeled and measured erythemal S_{ery} values ($f(x) = 0.93x + 113.45$ with x: measured values) and the correlation coefficient (0.96) reveal the good agreement between model and reality. The Mean Bias Error (MBE) of the model is −3 %, meaning that the model has a slight tendency to underestimate the measurements, which can be seen in Figs. 7 and 8. The Mean Absolute Bias Error (MABE), which is a useful measure to evaluate the overall performance of the model, equals 18 %. This means that the model proposed here, estimates the S_{ery} with a mean error of 18 %. Figure 7 and the upper panel of Fig. 8 show that in some cases, negative S_{ery} doses are modeled, which is a sign that the model does not always give realistic results. This is the case only during winter, when the S_g values are much lower than during the other seasons. When moderate to high Q_{O_3} values are combined with low S_g values, this leads to negative modeled S_{ery} values according to the regression equation. From Fig. 8 it is also clear that there is a seasonal cycle in the residual values. Therefore, it would be better to perform the multiple regression analysis on a seasonal scale.

4.4.2 Seasonal MLR analysis using total ozone column, global solar radiation and Aerosol Optical Depth

The multiple regression equations for the different seasons are presented below:

Spring:

$$S_{ery} = 1016 + 0.0001542 \times S_g - 5.660 \times Q_{O_3} + 92.11 \times \tau_{aer} + \epsilon \quad (7)$$

Summer:

$$S_{ery} = 2010 + 0.0001481 \times S_g - 6.737 \times Q_{O_3} - 134.2 \times \tau_{aer} + \epsilon \quad (8)$$

ACPD
14, 16529–16589, 2014

Autumn:

$$S_{ery} = -195 + 0.000143 \times S_g - 1.22 \times Q_{O_3} + 120 \times \tau_{aer} + \epsilon \quad (9)$$

Winter:

$$S_{ery} = 325 + 0.0000750 \times S_g - 1.50 \times Q_{O_3} + 101 \times \tau_{aer} + \epsilon \quad (10)$$

For all seasons, more than 80 % of the total variation in S_{ery} is explained by the combination of S_g, Q_{O_3} and τ_{aer}. This could be concluded from the adjusted R^2 values for each season. What might seem strange is the negative value of the constant term in the regression equation for autumn. However, the p value for this term is higher than 0.05, which means that this coefficient does not significantly differ from zero at the 95 % significance level.

From Fig. 9 and Table 9, it can be concluded that the seasonal models perform well in estimating the measured S_{ery} values. The correlation between the modeled and measured values varies between 0.90 (in winter) and 0.97 (in autumn). The regression equations are shown in both Fig. 9 and Table 9. The negative MBE values (except for autumn which has a value close to 0) show that each model has a tendency to underestimate the measured values. The summer model performs best with an absolute mean model error of only 6 %. The relative residuals (shown in Fig. 10) are smallest in summer, which again points out that the performance of the summer model in estimating the measured S_{ery} is the best. The spring and autumn models have much higher relative residuals.

Changes in the variation of S_g (Table 10) are the most important and lead to changes in erythemal UV dose between 18 % (in summer) and 53 % (in autumn). The influence of the variation in Q_{O_3} and τ_{aer} is much smaller. Changes in the variation of Q_{O_3} always lead to negative changes in S_{ery} (from −2 % in summer to −15 % in winter), whereas the influence of a change in variation of τ_{aer} varies from a negative value (−1 % change in S_{ery}) in summer to positive values in the other seasons, with a maximum of 4 % in winter

ACPD
14, 16529–16589, 2014

(Table 10). τ_{aer} and S_g have their lowest contribution in summer. Q_{O_3} on the other hand has the lowest contribution in autumn. The influence of Q_{O_3} is highest during winter and spring and this is in accordance with the variation in Q_{O_3} itself which is largest during winter and early spring. For τ_{aer} also, the absolute contribution to the variation in S_{ery} is the highest in winter. As the path length of UV irradiance is higher during winter, aerosols and ozone have more opportunity to influence UV irradiance on its way to the Earth's surface.

The influence of τ_{aer} on S_{ery} in the seasonal models is positive (except in summer) which is also the case when the τ_{aer} is used as the only explanatory variable in the models. This does not agree with what was observed in the trend analysis of the monthly anomalies time series, where an increase in erythemal UV dose is accompanied by a decrease in AOD. It has to be taken into account however, that the negative general AOD trend is not significant. Also, this negative trend in AOD is too much driven by the high, but sparse values at the beginning of the studied time period. Depending on the circumstances and the physical and optical properties of aerosols, the influence of AOD on global and UV irradiance can be either positive or negative. An increase in AOD could lead to an increase in global and UV radiation if the increase in AOD was caused by an increase in the amount of small scattering aerosol particles. These small particles would enhance the multiple scattering and reflection of UV irradiance, which in turn would increase the UV irradiance observed at the surface of the Earth. However, when the amount of small particles exceeded a certain (yet, herein not possible to determine) threshold value, extinction would take over and from this point, an increase in AOD would lead to a decrease in UV irradiance. Both the composition of aerosols (which determines whether a mixture is absorbing or scattering) and the size of the particles determine whether an increase in AOD will lead to either an increase or a decrease in UV irradiance. At Uccle, there is not sufficient information on both parameters to unambiguously characterize the influence of AOD on UV irradiance. Antón et al. (2011) already reported that it is hard to determine the effect of aerosols due to

ACPD
14, 16529–16589, 2014

their temporal and spatial variability and the difficulties associated with their characterization.

It has already been shown that S_g has the largest influence on S_{ery}, so an important issue that needs to be addressed is whether Q_{O_3} and τ_{aer} are actually necessary to capture the variation in S_{ery}. This was investigated by performing the MLR analysis using (1) only S_g, (2) S_g combined with Q_{O_3} and (3) S_g combined with τ_{aer} as explanatory variables. The adjusted R^2 value, the MABE and the correlation between modeled and measured S_{ery} values are given in Table 11. From these values, it becomes clear that τ_{aer} only has a minor contribution to the regression model and that to describe the changes in S_{ery}, τ_{aer} might not be needed, except perhaps for spring. It has to be taken into account that τ_{aer} is known to have an influence on S_g, hence it's influence on S_{ery} is already partly represented by the factor S_g. So we could say that τ_{aer} contributes in an indirect way, through S_g, to the variation in S_{ery}. It's direct contribution to S_{ery} only is negligible. For this reason it seems unnecessary to include τ_{aer} in the MLR analysis. Q_{O_3} seems to be a more important explanatory variable, as the adjusted R^2 increases for all seasons (except summer) and the MABE of the models decreases (except in summer) when combining S_g and Q_{O_3}. The correlation between modeled and measured values does not change much, except in winter (from 0.75 when using only S_g to 0.89 when combining S_g and Q_{O_3}).

5 Conclusions

Of the variables known to influence the UV irradiance that reaches the ground, the variability of global solar radiation, total ozone column and Aerosol Optical Depth (at 320.1 nm) are studied by performing a change-point analysis, a trend analysis and a multiple linear regression analysis. This is done in order to determine their changes over a 23 year time period (1991–2013) and their possible relation with the observed UV changes at Uccle, Belgium. The erythemal UV dose, TOC and AOD are measured

ACPD
14, 16529–16589, 2014

by the Brewer spectrophotometer instruments and the global solar radiation measurements are performed by a CM11 pyranometer.

For TOC and erythemal UV dose, a significant change point (or a significant shift in the mean of the monthly anomalies) was detected around February/March 1998, which has no known instrumental cause. The timing of the change point in ozone corresponds to results found in literature where studies define the change around this time period as the start of ozone recovery, following the regulations of the Montréal Protocol.

The trend over the past 23 years was determined for each variable using their monthly anomaly values. An overall positive trend was present in the time series of erythemal UV dose, global solar radiation and TOC of respectively +7 % (±2 %), +4 % (±1 %) and +2.6 % (±0.4 %) per decade. In contrast, the trend of AOD, equal to −8 % (±5 %) per decade, is (insignificantly) negative over the investigated time period. The sign and magnitude of the trends observed at Uccle agree with results found in literature for stations of comparable latitude. The increase in global solar radiation since 1991 could be interpreted as a sign of continuing global brightening over Belgium. The decrease in sulfur and black carbon emissions after 1989, which resulted in enhanced global solar radiation at the Earth's surface, is most probably also the driving mechanism for the decrease in AOD, which in turn could have an influence by increasing the UV irradiance.

For both erythemal UV dose and global solar radiation, there is an increase in the frequency of higher values towards the second part of the study period (2003–2013), without the entire frequency distribution shifting. This could be explained by a decrease in cloudiness towards 2003–2013. Several studies report on a decrease in cloud cover over the past decades and a tendency for cumuliform clouds to replace stratiform clouds (Norris and Slingo, 2009; Eastman and Warren, 2013). This would increase both global solar radiation and UV irradiance due to enhanced scattering. However, other parameters (such as ozone and aerosols) could also influence the values of erythemal UV dose and global solar radiation. As opposed to erythemal UV dose and global solar radiation, a clear shift can be seen in the entire frequency distribution of

ACPD
14, 16529–16589, 2014

daily TOC values, with both minimum and maximum values having increased from the 1991–2002 period to the 2003–2013 period, which supports literature findings about an ozone recovery around the end of the 1990s. From the frequency distribution of daily AOD values, it can be derived that between 1991 and 2002, higher AODs were more frequently present than during the last period (2003–2013), which is in agreement with the overall decrease over the last 23 years.

The seasonal trends of the four variables were also studied and are similar between erythemal UV dose and global solar radiation, with a positive trend for all seasons except winter. The TOC trend is positive for spring and summer. Normally, we would expect a positive TOC trend to be accompanied with a negative trend in erythemal UV dose. The fact that the observed trends have the same sign, could indicate that the change in UV irradiance is not only influenced by a change in total ozone values. The AOD trend is negative during summer and autumn. The trend in spring is not significant and not enough winter data were present to calculate a winter trend.

To investigate the influences of global solar radiation, TOC and AOD on the erythemal UV dose, a multiple linear regression was performed using daily values between 1991 and 2008. The three variables together explain 94 % of the total variation in the observed erythemal UV dose. Global solar radiation has the largest influence on the erythemal UV dose, followed by TOC and AOD. Data of 2009–2013 were used to validate the model and the MBA and MABE were calculated to evaluate the model performance in terms of overestimation and average error. The MBE value of the model is −3 %, which means that the model has a slight tendency to underestimate the measured UV irradiance values. The average error of the model in the estimation of the measurements is equal to 18 %. Overall, the model represents reality well, however sometimes (only during winter) negative erythemal UV dose values were modeled. For this reason, seasonal regression models have been developed.

All seasonal models perform rather well in explaining the variation in UV irradiance (with adjusted R^2 values larger than 0.8). The negative MBE values show the models' tendencies to underestimate UV irradiance. Again, global solar radiation has the largest

ACPD
14, 16529–16589, 2014

influence on erythemal UV dose, followed by TOC and AOD. The summer regression model performs best, based on the very low MABE values.

What is seen in reality (i.e. an increase in erythemal UV dose accompanied with an increase in TOC and a decrease in AOD) is not always what is represented by the models. According to the regression models, TOC and AOD respectively always have a negative and positive influence on erythemal UV dose. However, as global solar radiation is obviously the most important factor in explaining the variation in erythemal UV dose, the increase in TOC (which would be expected to lead to a decrease in erythemal UV dose) and the change in AOD seem to be compensated for by the increase in global radiation.

The question that remains is whether TOC and AOD are needed as explanatory variables in the multiple linear regression models. It has been shown that the contribution of AOD to explaining the variation in erythemal UV dose is very small and it can be concluded that this variable is not really needed in the multiple linear regression model. Also its influence is already partly represented by the global radiation parameter. Total ozone column however, does seem to be a more important factor in capturing the variation in erythemal UV dose and cannot be discarded from the regression models.

Acknowledgements. This research was performed under the project AGACC-II contract SD/CS/07A of the Belgian Science Policy. We thank C. Hermans (Belgian Institute for Space Aeronomy, Belgium) for establishing and maintaining the AERONET site at Uccle.

References

Alpert, P., Shvainshtein, O., and Kishcha, P.: AOD trends over megacities based on space monitoring using MODIS and MISR, American Journal of Climate Change, 1, 117–131, doi:10.4236/ajcc.2012.13010, 2012. 16550, 16576

Antón, M., Serrano, A., Cancillo, M. L., and García, J. A.: An empirical model to estimate ultraviolet erythemal transmissivity, Ann. Geophys., 27, 1387–1398, doi:10.5194/angeo-27-1387-2009, 2009. 16533, 16542

ACPD
14, 16529–16589, 2014

Antón, M., Gil, J. E., Fernández-Gálvez, J., Lyamani, H., Valenzuela, A., Foyo-Moreno, I., Olmo, F. J., and Alados-Arboledas, L.: Evaluation of the aerosol forcing efficiency in the UV erythemal range at Granada, Spain, J. Geophys. Res., 116, D20214, doi:10.1029/2011JD016112, 2011. 16554

Augustine, J. A., Hodges, G. B., Dutton, E. G., Michalsku, J. J., and Cornwall, C. R.: An aerosol optical depth climatology for NOAA's national surface radiation budget network (SURFRAD), J. Geophys. Res., 113, D11204, doi:10.1029/2007JD009504, 2008. 16550

Bais, A. F., Kazadzis, S., Meleti, C., Kouremeti, N., Kaurola, J., Lakkala, K., Slaper, H., den Outer, P. N., Josefsson, W., Feister, U., and Janouch, M.: Variability in spectral UV irradiance at seven European stations, in: Proceedings of the UV Conference, One Century of UV Radiation Research, edited by: Gröbner, J., Davos, Switzerland, 18–20 September 2007, 1:27, 2007. 16574

Bais, A. F., Tourpali, K., Kazantzidis, A., Akiyoshi, H., Bekki, S., Braesicke, P., Chipperfield, M. P., Dameris, M., Eyring, V., Garny, H., Iachetti, D., Jöckel, P., Kubin, A., Langematz, U., Mancini, E., Michou, M., Morgenstern, O., Nakamura, T., Newman, P. A., Pitari, G., Plummer, D. A., Rozanov, E., Shepherd, T. G., Shibata, K., Tian, W., and Yamashita, Y.: Projections of UV radiation changes in the 21st century: impact of ozone recovery and cloud effects, Atmos. Chem. Phys., 11, 7533–7545, doi:10.5194/acp-11-7533-2011, 2011. 16532, 16549

Bartlett, L. M. and Webb, A. R.: Changes in ultraviolet radiation in the 1990s: spectral measurements from Reading, England, J. Geophys. Res., 105, 4889–4893, doi:10.1029/1999JD900493, 2000. 16531, 16549, 16575

Bernhard, G., Booth, C. R., Ehramjian, J. C., and Nichol, S. E.: UV climatology at McMurdo Station, Antarctica, based on Version 2 data of the National Science Foundation's Ultraviolet Radiation Monitoring Network, J. Geophys. Res., 111, D11201, doi:10.1029/2005JD005857, 2006. 16532

Bernhard, G.: Trends of solar ultraviolet irradiance at Barrow, Alaska, and the effect of measurement uncertainties on trend detection, Atmos. Chem. Phys., 11, 13029–13045, doi:10.5194/acp-11-13029-2011, 2011. 16532, 16533

Bojkov, R. D., Bishop, L., and Fioletov, V.: Total ozone trends from quality-controlled ground-based data (1964–1994), J. Geophys. Res., 100, 25867–25876, 1995. 16549, 16575

ACPD
14, 16529–16589, 2014

Cheymol, A. and De Backer, H.: Retrieval of the aerosol optical depth in the UV-B at Uccle from Brewer ozone measurements over a long time period 1984–2002, J. Geophys. Res., 108, 4800, doi:10.1029/2003JD003758, 2003. 16536

Chiaccio, M., Ewen, T., Wild, M., Chin, M., and Diehl, T.: Decadal variability of aerosol optical depth in Europe and its relationship to the temporal shift of the North Atlantic Oscillation in the realm of dimming and brightening, J. Geophys. Res., 116, D02108, doi:10.1029/2010JD014471, 2011. 16550

Chubarova, N. Y.: UV variability in Moscow according to long-term UV measurements and reconstruction model, Atmos. Chem. Phys., 8, 3025–3031, doi:10.5194/acp-8-3025-2008, 2008. 16532, 16574

Cordero, R. R., Seckmeyer, G., Pissulla, D., and Labbe, F.: Exploitation of spectral direct UV irradiance measurements, Metrologia, 46, 19–25, doi:10.1088/0026-1394/46/1/003, 2009. 16532

De Backer, H. and De Muer, D.: Intercomparison of total ozone data measured with Dobson and Brewer ozone spectrophotometers at Uccle (Belgium) from January 1984 to March 1991, including zenith sky observations, J. Geophys. Res., 96, 20711–20719, 1991. 16536

De Backer, H.: Time series of daily erythemal UV doses at Uccle, Belgium, Int. J. Remote Sens., 30, 4145–4145, doi:10.1080/01431160902825032, 2009. 16533, 16534

De Bock, V., De Backer, H., Mangold, A., and Delcloo, A.: Aerosol Optical Depth measurements at 340 nm with a Brewer spectrophotometer and comparison with Cimel sunphotometer observations at Uccle, Belgium, Atmos. Meas. Tech., 3, 1577–1588, doi:10.5194/amt-3-1577-2010, 2010. 16536

de la Casinière, A., Lamine Touré, M., Masserot, D., Cabot, T., and Pinedo Vega, J. L.: Daily doses of biologically active UV radiation retrieved from commonly available parameters, Photochem. Photobiol., 76, 171–175, 2002. 16533

De Meij, A., Pozzer, A., and Lelieveld, J.: Trend analysis in aerosol optical depths and pollutant emission estimates between 2000 and 2009, Atmos. Environ., 51, 75–85, doi:10.1016/j.atmosenv.2012.01.059, 2012. 16550

den Outer, P. N., Slaper, H., Matthijsen, J., Reinen, H. A. J. M., and Tax, R.: Variability of ground-level ultraviolet: Model and Measurement, Radiat. Prot. Dos., 91, 105–110, 2000. 16532

den Outer, P. N., Slaper, H., Kaurola, J., Lindfors, A., Kazantzidis, A., Bais, A. F., Feister, U., Junk, J., Janouch, M., and Josefsson, W.: Reconstructing of erythemal ultravio-

ACPD
14, 16529–16589, 2014

let radiation levels in Europe for the past 4 decades, J. Geophys. Res., 115, D10102, doi:10.1029/2009JD012827, 2010. 16532, 16574
Díaz, S., Deferrari, G., Martinioni, D., and Oberto, A.: Regression analysis of biologically effective integrated irradiances versus ozone, clouds and geometric factors, J. Atmos. Sol.-Terr. Phy., 62, 629–638, 2000. 16533
Diffey, B. L.: Solar ultraviolet radiation effects on biological systems, Phys. Med. Biol., 36, 299–328, doi:10.1088/0031-9155/36/3/001, 1991. 16532
Durbin, J. and Watson, G. S.: Testing for serial correlation in least squares regression III, Biometrika, 58, 1–19, 1971. 16540
Eastman, R. and Warren, S. G.: A 39-yr survey of cloud changes from land stations worldwide 1971–2009: long-term trends, relation to aerosol and expansion of the tropical belt, J. Climate, 26, 1286–1303, doi:10.1175/JCLI-D-12-00280.1, 2013. 16556
Eck, T. F., Holben, B. N., Reid, J. S., Dubovik, O., Smirnov, A., O'Neill, N. T., Slutsker, I., and Kinne, S.: Wavelength dependence of the optical depth of biomass burning, urban, and desert dust aerosols, J. Geophys. Res., 104, 31333–31349, doi:10.1029/1999JD900923, 1999. 16538
El Shazly, S. M., Kassem, Kh. O., Hassan, A. A., and El-Nobi, A. F.: An empirical model to estimate UV index in some upper Egypt regions, Resources and Environment, 2, 216–227, doi:10.5923/j.re.20120205.05, 2012. 16533
Fioletov, V. E., McArthur, L. J. B., Kerr, J. B., and Wardle, D. I.: Long-term variations of UV-B irradiance over Canada estimated from Brewer observations and derived from ozone and pyranometers measurements, J. Geophys. Res., 106, 23009–23027, 2001. 16533
Fioletov, V. E., Kerr, J. B., Wardle, D. I., Krotkov, N., and Herman, J. R.: Comparison of Brewer ultraviolet irradiance measurements with total ozone mapping spectrometer satellite retrievals, Opt. Eng., 41, 3051–3061, doi:10.1117/1.1516818, 2002. 16534
Fioletov, V. E., Kimlin, M. G., Krotkov, N., McArthur, L. J. B., Kerr, J. B., Wardle, D. I., Herman, J. R., Meltzer, R., Mathews, T. W., and Kaurola, J.: UV index climatology over the United States and Canada from ground-based and satellite estimates, J. Geophys. Res., 109, D22308, doi:10.1029/2004JD004820, 2004. 16532
Fitzka, M., Simic, S., and Hadzimustafic, J.: Trends in spectral UV radiation from long-term measurements at Hoher Sonnblick, Austria, Theor. Appl. Climatol., 110, 585–593, doi:10.1007/s00704-012-0684-0, 2012. 16531, 16532, 16533, 16549, 16574, 16575, 16576

ACPD
14, 16529–16589, 2014

Foyo-Moreno, I., Alados, I., and Alados-Arboledas, L.: Adaptation of an empirical model for erythemal ultraviolet irradiance, Ann. Geophys., 25, 1499–1508, doi:10.5194/angeo-25-1499-2007, 2007. 16533

Garane, K., Bais, A. F., Kazadzis, S., Kazantzidis, A., and Meleti, C.: Monitoring of UV spectral irradiance at Thessaloniki (1990–2005): data re-evaluation and quality control, Ann. Geophys., 24, 3215–3228, doi:10.5194/angeo-24-3215-2006, 2006. 16531

Glandorf, M., Arola, A., Bais, A., and Seckmeyer, G.: Possibilities to detect trends in spectral UV irradiance, Theor. Appl. Climatol., 88, 33–44, doi:10.1007/s00704-004-0109-9, 2005. 16533, 16549, 16575

Gröbner, J. and Meleti, C.: Aerosol optical depth in the UVB and visible wavelength range from Brewer spectrophotometer direct irradiance measurements: 1991–2002, J. Geophys. Res., 109, D09202, doi:10.1029/2003JD004409, 2004. 16536

Gröbner, J., Kazadzis, S., Schreder, J., Bolsée, D., Brogniez, C., De Backer, H., di Sarra, A.G., Feister, U., Görts, P., Henriques, D., Jaroslawski, J., Simic, S., Stanec, M., Steinmetz, M., Tax, R., and Vilaplana Guerrero, J. M.: Quality assurance of spectral ultraviolet measurements in Europe throught the development of a transportable unit (QASUME) – Round of site visits 2004, European Commission (Joint Research Centre), Ispra (Italy), EUR 21398 EN, 171–182, 2004. 16535

Harris, N. R. P., Kyrö, E., Staehelin, J., Brunner, D., Andersen, S.-B., Godin-Beekmann, S., Dhomse, S., Hadjinicolaou, P., Hansen, G., Isaksen, I., Jrrar, A., Karpetchko, A., Kivi, R., Knudsen, B., Krizan, P., Lastovicka, J., Maeder, J., Orsolini, Y., Pyle, J. A., Rex, M., Vanicek, K., Weber, M., Wohltmann, I., Zanis, P., and Zerefos, C.: Ozone trends at northern mid- and high latitudes – a European perspective, Ann. Geophys., 26, 1207–1220, doi:10.5194/angeo-26-1207-2008, 2008. 16549

Herman, J. R., Bhartia, P. K., Ziemke, J., Ahmad, Z., and Larko, D.: UV-B increases (1979–1992) from decreases in total ozone, Geophys. Res. Lett., 23, 2117–2120, 1996. 16532

Herman, J. R.: Global increase in UV irradiance during the past 30 years (1979–2008) estimated from satellite data, J. Geophys. Res., 115, D04203, doi:10.1029/2009JD012219, 2010. 16549

Holben, B. N., Tanré, D., Smirnov, A., Eck, T. F., Slutsker, I., Abuhassan, N., Newcomb, W. W., Schafer, J. S., Chatenet, B., Lavenu, F., Kaufman, Y. J., Vande Castle, J., Setzer, A., Markham, B., Clark, D., Frouin, R., Halthore, R., Karneli, A., O'Neill, N. T., Pietras, C., Pinker, R. T., Voss, K., and Zibordi, G.: An emerging ground-based aerosol

ACPD
14, 16529–16589, 2014

climatology: aerosol optical depth from AERONET, J. Geophys. Res., 106, 12067–12097, doi:10.1029/2001JD900014, 2001. 16538
Hoppe, H. and Kiely, G.: Precipitation over Ireland: observed change since 1940, Phys. Chem. Earth B, 24, 91–96, 1999. 16539
Hsu, N. C., Gautam, R., Sayer, A. M., Bettenhausen, C., Li, C., Jeong, M. J., Tsay, S.-C., and Holben, B. N.: Global and regional trends of aerosol optical depth over land and ocean using SeaWiFS measurements from 1997 to 2010, Atmos. Chem. Phys., 12, 8037–8053, doi:10.5194/acp-12-8037-2012, 2012. 16550
Huang, M., Jiang, H., Ju, W., and Xiao, Z.: Ultraviolet radiation over two lakes in the Middle and lower reaches of the Yangtze river, China: an innovative model for UV estimation, Terr. Atmos. Ocean. Sci., 22, 491–506, doi:10.3319/TAO.2011.05.02.01(A), 2011. 16533
Journée, M. and Bertrand, C.: Improving the spatio-temporal distribution of surface solar radiation data by merging ground and satellite measurements, Remote Sens. environ., 114, 2692–2704, doi:10.1016/j.rse.2010.06.010, 2010. 16535
Kalliskota, S., Kaurola, J., Taalas, P., Herman, J., Celarier, E. A., and Krotkov, N. A.: Comparison of daily UV doses estimated from Nimbus 7/TOMS measurements and ground-based spectroradiometric data, J. Geophys. Res., 105, 5059–5067, 2000. 16532
Kaurola, J., Taalas, P., Koskela, T., Borkowsko, J., and Josefsson, W.: Long-term variations of UV-B doses at three stations in northern Europe, J. Geophys. Res., 105, D16, 20813–20820, 2000. 16531, 16532
Kazadzis, S., Bais, A., Amiridis, V., Balis, D., Meleti, C., Kouremeti, N., Zerefos, C. S., Rapsomanikis, S., Petrakakis, M., Kelesis, A., Tzoumaka, P., and Kelektsoglou, K.: Nine years of UV aerosol optical depth measurements at Thessaloniki, Greece, Atmos. Chem. Phys., 7, 2091–2101, doi:10.5194/acp-7-2091-2007, 2007. 16576
Krishna Prasad, N. V., Niranjan, K., Sarma, M. S. S. R. K., and Madhavi, N.: Regression analysis of biologically effective UV-B irradiance versus ozone at Visakhapatnam, Int. J. Phys. Sci., 6, 7838–7843, doi:10.5897/IJPS11.581, 2011. 16533, 16541
Krzyścin, J. W. and Borkowski, J. L.: Variability of the total ozone trend over Europe for the period 1950–2004 derived from reconstructed data, Atmos. Chem. Phys., 8, 2847–2857, doi:10.5194/acp-8-2847-2008, 2008. 16549
Krzyścin, J. W., Sobolweski, P. S., Jaroslawski, J., Podgórski, J., and Rajewska-Wiech, B.: Erythemal UV observations at Belsk, Poland, in the period 1976–2008: data homogeniza-

ACPD
14, 16529–16589, 2014

tion, climatology and trends, Acta Geophys., 59, 155–182, doi:10.2478/s11600-010-0036-3, 2011. 16531, 16533, 16574
Lanzante, J. R.: Resistant, Robust and Non-parametric techniques for the analysis of climate data: theory and examples, including applications to historical radiosonde station data, Int. J. Climatol., 16, 1197–1226, 1996. 16539
Litynska, Z., Koepke, P., De Backer, H., Gröbner, J., Schmalwieser, A., and Vuilleumier, L.: COST action 726 final report: Long term changes and climatology of UV radiation over Europe, ISBN 978-92-898-0052-5, Publications office of the European Union, Luxembourg, 2012. 16548
Makowski, K., Jaeger, E. B., Chiacchio, M., Wild, M., Ewen, T., and Ohmura, A.: On the relationship between diurnal temperature range and surface solar radiation in Europe, J. Geophys. Res., 114, D00D07, doi:10.1029/2008JD011104, 2009. 16548
Matthijsen, J., Slaper, H., Reinen, A. J. M. H., and Velders, G. J. M.: Reduction of solar UV by clouds: a comparison between satellite-derived cloud effects and ground-based radiation measurements, J. Geophys. Res., 105, 5069–5080, 2000. 16532
Mishchenko, M. I. and Geogdzhayev, I. G.: Satellite remote sensing reveals regional tropospheric aerosol trends, Opt. Express, 15, 7423–7438, 2007. 16550
Nabat, P., Somot, S., Mallet, M., Chiapello, I., Morcrette, J. J., Solmon, F., Szopa, S., Dulac, F., Collins, W., Ghan, S., Horowitz, L. W., Lamarque, J. F., Lee, Y. H., Naik, V., Nagashima, T., Shindell, D., and Skeie, R.: A 4-D climatology (1979–2009) of the monthly tropospheric aerosol optical depth distribution over the Mediterranean region from a comparative evaluation and blending of remote sensing and model products, Atmos. Meas. Tech., 6, 1287–1314, doi:10.5194/amt-6-1287-2013, 2013. 16550
Norris, J. R. and Slingo, A.: Trends in observed cloudiness and earth's radiation budget, in: Clouds in the Perturbed Climate System: Their Relationship to Energy Balance, Atmospheric Dynamics and Precipitation, edited by: Heintzenberg, J., and Charlson, R. J., chap. 2, MIT Press, Cambridge, MA, USA, 17–36, 2009. 16556
Norris, J. R. and Wild, M.: Trends in aerosol radiative effects over Europe inferred from observed cloud cover, solar "dimming", and solar "brightening", J. Geophys. Res., 112, D08214, doi:10.1029/2006JD007794, 2007. 16548
Nyeki, S., Halios, C. H., Baum, W., Eleftheriadis, K., Flentje, H., Gröbner, J., Vuilleumier, L., and Wehrli, C.: Ground-based aerosol optical depth trends at three high-altitude sites in

ACPD
14, 16529–16589, 2014

Switzerland and southern Germany from 1995 to 2010, J. Geophys. Res., 117, D18202, doi:10.1029/2012JD017493, 2012. 16576

Reeves, J., Chen, J., Wang, X. L., Lund, R., and Lu, Q.: A review and comparison of changepoint detection techniques for climate data, J. Appl. Meteorol. Clim., 46, 900–915, doi:10.1175/JAM2493.1, 2007.

Reinsel, G.C, Miller, A. J., Weatherhead, E. C., Flynn, L. E., Nagatani, R. M., Tiao, G., and Wuebbles, D. J.: Trend analysis of total ozone data for turnaround and dynamical contributions, J. Geophys. Res., 110, D16306, doi:10.1029/2004JD004662, 2005. 16544

Rieder, H. E., Holawe, F., Simic, S., Blumthaler, M., Krzyścin, J. W., Wagner, J. E., Schmalwieser, A. W., and Weihs, P.: Reconstruction of erythemal UV-doses for two stations in Austria: a comparison between alpine and urban regions, Atmos. Chem. Phys., 8, 6309–6323, doi:10.5194/acp-8-6309-2008, 2008. 16532

Rieder, H. E., Staehelin, J., Weihs, P., Vuillemier, L., Maeder, J. A., Holwae, F., Blumthaler, M., Lindfors, A., Peter, T., Simic, S., Spichtinger, P., Wagner, J. E., Walker, D., and Ribatet, M.: Relationship between high daily erythemal UV doses, total ozone, surface albedo and cloudiness: An analysis of 30 years of data from Switzerland and Austria, Atmos. Res., 98, 9–20, 2010. 16532, 16533

Rieder, H. E., Frossard, L., Ribatet, M., Staehelin, J., Maeder, J. A., Di Rocco, S., Davison, A. C., Peter, T., Weihs, P., and Holawe, F.: On the relationship between total ozone and atmospheric dynamics and chemistry at mid-latitudes – Part 2: The effects of the El Niño/Southern Oscillation, volcanic eruptions and contributions of atmospheric dynamics and chemistry to long-term total ozone changes, Atmos. Chem. Phys., 13, 165–179, doi:10.5194/acp-13-165-2013, 2013. 16549

Sanchez-Lorenzo, A. and Wild, M.: Decadal variations in estimated surface solar radiation over Switzerland since the late 19th century, Atmos. Chem. Phys., 12, 8635–8644, doi:10.5194/acp-12-8635-2012, 2012. 16548

Santer, B. D., Wigley, T. M. L., Boyle, J. S., Gaffen, D. J., Hnilo, J. J., Nychka, D., Parker, D. E., and Taylor, K. E.: Statistical significance of trends and trend differences in layer-average atmospheric temperature time series, J. Geophys. Res., 105, 7337–7356, 2000. 16539, 16540

Sasaki, M., Takeshita, S., Oyanagi, T., Miyake, Y., and Sakata, T.: Increasing trend of biologically active solar ultraviolet-B irradiance in mid-latitude Japan in the 1990s, Opt. Eng., 41, 3062–3069, 2002. 16532

ACPD
14, 16529–16589, 2014

SCI TEC: Brewer Ozone Spectrophotometer, Acceptance manual, Document number AM-BA-CO5-Rev C, Sci. Tec. Instruments, Saskatoon, Saskatchewan, Canada, 1988. 16534
Smedley, A. R. D., Rimmer, J. S., Moore, D., Roumi, R., and Webb, A. R.: Total ozone and surface UV trends in the United Kingdom: 1979–2008, Int. J. Climatol., 32, 338–346, doi:10.1002/joc.2275, 2012. 16531, 16549, 16574, 16575
Solomon, S., Qin, D., Manning, M., Chen, Z., Marquis, M., Averyt, K. B., Tignor, M., and Miller, H. L. (Eds.): Intergovernmental Panel on Climate Change 2007: The physical science, Technical summary of the working group I report, Cambridge University Press, New York, 2007. 16548
Staehelin, J., Kegel, R., and Harris, N. R. P.: Trend analysis of the homogenized total ozone series of Arosa (Switzerland) 1926–1996, J. Geophys. Res., 103, 8389–8399, 1998. 16549, 16575
Steinbrecht, W., Claude, H., Schönenborn, F., McDermid, I. S., Leblanc, T., Godin, S., Song, T., Swart, D. P. J., Meijer, Y. J., Bodeker, G. E., Connor, B. J., Kämpfer, N., Hocke, K., Calisesi, Y., Schneider, N., de la Noë, J., Parrish, A. D., Boyd, I. S., Brühl, C., Steil, B., Giorgetta, M. A., Manzini, E., Thomason, L. W., Zawodny, J. M., McCormick, M. P., Russell III, J. M., Bhartia, P. K., Stolarski, R. S., and Hollandsworth-Frith, S. M.: Long-term evolution of upper stratospheric ozone at selected stations of the Network for the Detection of Stratospheric Change (NDSC), J. Geophys. Res., 111, D1027, doi:10.1029/2005JD006454, 2006. 16544, 16549
Stjern, C. W., Egill Kristjánsson, J., and Hansen, A. W.: Global dimming and global brightening: an analysis of surface radiation and cloud cover data in northern Europe, Int. J. Climatol., 29, 643–653, doi:10.1002/joc.1735, 2009. 16548
Tevini, M. and Teramura, H. A.: UV-B effects on terrestrial plants, Photochem. Photobiol., 50, 479–487, doi:10.1111/j.1751-1097.1989.tb05552.x, 1989. 16532
Trepte, S. and Winkler, P.: Reconstruction of erythemal UV irradiance and dose at Hohenpeissenberg (1968–2001) considering trends of total ozone, cloudiness and turbidity, Theor. Appl. Climatol., 77, 159–171, doi:10.1007/s00704-004-0034-y, 2004. 16532
Van Malderen, R. and De Backer, H.: A drop in upper tropospheric humidity in autumn 2001, as derived from radiosonde measurements at Uccle, Belgium, J. Geophys. Res., 115, D20114, doi:10.1029/2009JD013587, 2010. 16538
Vigouroux, C., De Mazière, M., Demoulin, P., Servais, C., Hase, F., Blumenstock, T., Kramer, I., Schneider, M., Mellqvist, J., Strandberg, A., Velazco, V., Notholt, J., Sussmann, R.,

ACPD
14, 16529–16589, 2014

Stremme, W., Rockmann, A., Gardiner, T., Coleman, M., and Woods, P.: Evaluation of tropospheric and stratospheric ozone trends over Western Europe from ground-based FTIR network observations, Atmos. Chem. Phys., 8, 6865–6886, doi:10.5194/acp-8-6865-2008, 2008. 16549, 16575

Weatherhead, C. E., Reinsel., G. C., Tiao, G. C., Meng, X.-L., Choi, D., Cheang, W.-K., Keller, T., DeKuisi, J., Wuebbles, D. J., Kerr, J. B., Miller, A. J., Oltmans, S. J., and Frederick, J. E.: Factors affecting the detection of trends: Statistical considerations and applications to environmental data, J. Geophys. Res., 103, 17149–17161, 1998. 16533

Wenny, B. N., Saxena, V. K., and Frederick, J. E.: Aerosol optical depth measurements and their impact on surface levels of ultraviolet-B radiation, J. Geophys. Res., 106, 17311–17319, 2001. 16544

Wild, M., Trüssel, B., Ohmura, A., Long, C. N., König-Langlo, G., Dutton, E. G., and Tsvetkov, A.: Global dimming and brightening: an update beyond 2000, J. Geophys. Res., 114, D00D13, doi:10.1029/2008JD011382, 2009. 16548, 16550

Williams, J. E., den Outer, P. N., Slaper, H., Matthijsen, J., and Kelfkens, G.: Cloud induced reduction of solar UV-radiation: a comparison of ground-based and satellite based approaches, Geophys. Res. Lett., 31, L03104, doi:10.1029/2003GL018242, 2004. 16532

WMO (World Meteorological Organization), Scientific Assessment of Ozone Depletion: 2006, Global Ozone Research and Monitoring Project-Report No. 50, 572 pp., Geneva, Switzerland, 2007 16531

Zerefos, C. S., Balis, D. S., Bais, A. F., Gillotay, D., Simon, P. C., Mayer, B., and Seckmeyer, G.: Variability of UV-B at four stations in Europe, Geophys. Res. Lett., 24, 1363–1366, 1997. 16549, 16575

Zerefos, C., Balis, D., Tzortziou, M., Bais, A., Tourpali, K., Meleti, C., Bernhard, G., and Herman, J.: A note on the interannual variations of UV-B erythemal doses and solar irradiance from ground-based and satellite observations, Ann. Geophys., 19, 115–120, doi:10.5194/angeo-19-115-2001, 2001. 16532

Zerefos, C. S., Tourpali, K., Eleftheratos, K., Kazadzis, S., Meleti, C., Feister, U., Koskela, T., and Heikkilä, A.: Evidence of a possible turning point in solar UV-B over Canada, Europe and Japan, Atmos. Chem. Phys., 12, 2469–2477, doi:10.5194/acp-12-2469-2012, 2012. 16532, 16547, 16550

ACPD
14, 16529–16589, 2014

Ziemke, J. R., Chandra, S., Herman, J., and Varotsos, C.: Erythemally weighted UV trends over northern latitudes derived from Nimbus 7 TOMS measurements, J. Geophys. Res., 105, 7373–7382, 2000. 16532

ACPD
14, 16529–16589, 2014

Table 1. Comparison of Brewer and Cimel AOD values (2006–2013).

		Correlation	Slope	Intercept
DS 320 nm	Brewer#016	0.97	1.004 ± 0.006	−0.067 ± 0.003
DS 320 nm	Brewer#178	0.99	1.007 ± 0.005	0.017 ± 0.002
SS 340 nm	Brewer#178	0.98	0.993 ± 0.007	0.073 ± 0.002

ACPD
14, 16529–16589, 2014

Table 2. Seasonal trends of erythemal UV doses (1991–2013).

Season	Trend per decade	Significance level
Spring	+9 %(±3 %)	99 %
Summer	+6 %(±2 %)	99 %
Autumn	+7 %(±3 %)	95 %
Winter	−12 %(±4 %)	99 %

ACPD
14, 16529–16589, 2014

Table 3. Seasonal trends of global solar radiation (1991–2013).

Season	Trend per decade	Significance level
Spring	+6 %(±3 %)	95 %
Summer	+2 %(±2 %)	not significant
Autumn	+6 %(±3 %)	95 %
Winter	−4 %(±4 %)	not significant

ACPD
14, 16529–16589, 2014

Table 4. Seasonal trends of total ozone (1991–2013).

Season	Trend per decade	Significance level
Spring	+3 %(±1 %)	95 %
Summer	+1.6 %(±0.6 %)	95 %
Autumn	+1.8 %(±0.9 %)	not significant
Winter	+3 %(±2 %)	not significant

ACPD
14, 16529–16589, 2014

Table 5. Seasonal trends of AOD at 320.1 nm (1991–2013).

Season	Trend per decade	Significance level
Spring	+2 %(±7 %)	not significant
Summer	−18 %(±8 %)	95 %
Autumn	−36 %(±14 %)	95 %
Winter	Not enough data	

ACPD
14, 16529–16589, 2014

Table 6. Trends of UV radiation at different stations from (a): Bais et al. (2007), (b): Krzyścin et al. (2011), (c): Smedley et al. (2012), (d): Fitzka et al. (2012), (e): den Outer et al. (2010) and (f): Chubarova (2008).

Station, Country	Latitude/Longitude	Period	Trend/decade	Reference
Measured UV trends				
Sodankylä, Finland	67.42° N/26.59° E	1990–2004	+2.1 % (60° SZA)	(a)
Jokioinen, Finland	60.80° N/23.49° E	1996–2005	−1.9 % (60° SZA)	(a)
Norrköping, Sweden	58.36° N/16.12° E	1996–2004	+12 % (60° SZA)	(a)
Bilthoven, the Netherlands	52.13° N/5.20° E	1996–2004	+8.6 % (60° SZA)	(a)
Belsk, Poland	51.83° N/20.81° E	1976–2008	+5.6 %	(b)
Reading, UK	51.45° N/0.98° W	1993–2008	+6.6 %	(c)
Hradec Kralove, Czech Rep.	50.21° N/15.82° E	1994–2005	−2.1 % (60° SZA)	(a)
Lindenberg, Germany	47.60° N/9.89° E	1996–2003	+7.7 % (60° SZA)	(a)
Hoher Sonnblick, Austria	47.05° N/12.96° E	1997–2011	+14.2 % (65° SZA)	(d)
Thessaloniki, Greece	40.63° N/22.95° E	1990–2004	+3.4 % (60° SZA)	(a)
Reconstructed or Modeled UV trends				
Sodankylä, Finland	67.42° N/26.59° E	1980–2006	+3.6 %	(e)
Jokioinen, Finland	60.80° N/23.49° E	1980–2006	+2.8 %	(e)
Norrköping, Sweden	58.36° N/16.12° E	1980–2006	+4.1 %	(e)
Moscow, Russia	55.75° N/37.62° E	1980–2006	+6 %	(f)
Bilthoven, the Netherlands	52.13° N/5.20° E	1980–2006	+2.9 %	(e)
Hradec Kralove, Czech Rep.	50.21° N/15.82° E	1980–2006	+5.2 %	(e)
Lindenberg, Germany	47.60° N/9.89° E	1980–2006	+5.8 %	(e)
Thessaloniki, Greece	40.63° N/22.95° E	1980–2006	+4.4 %	(e)

ACPD
14, 16529–16589, 2014

Table 7. Trends of total ozone at different stations from (a): Glandorf et al. (2005), (b): Smedley et al. (2012), (c): Bartlett and Webb (2000), (d): Bojkov et al. (1995), (e): Zerefos et al. (1997), (f): Fitzka et al. (2012), (g): Staehelin et al. (1998) and (h): Vigouroux et al. (2008).

Station, Country	Latitude/Longitude	Period	Trend/decade	Reference
Sodankylä, Finland	67.42° N/26.59° E	1979–1998	−5.7 %	(a)
Lerwick, UK	60.15° N/1.15° W	1979–1993	−5.8 %	(b)
Reading, UK	51.45° N/0.98° W	1993–1997	−5.9 %	(c)
Brussels, Belgium	50.84° N/4.36° E	1971–1994	−2.6 %	(d)
Brussels, Belgium	idem	1993–1996	−15.0 %	(e)
Hradec Kralove, Czech Rep.	50.21° N/15.82° E	1994–2005	−2.2 %	(d)
Hohenpeisenberg, Germany	47.80° N/11.00° E	1968–1994	−3.5 %	(d)
Hoher Sonnblick, Austria	47.05° N/12.96° E	1997–2011	+1.9 %	(f)
Arosa, Switzerland	46.77° N/9.67° E	1964–1994	−2.7 %	(d)
Arosa, Switzerland	idem	1970–1996	−2.3 %	(g)
Jungfraujoch, Switzerland	46.55° N/7.98° E	1995–2004	+4.1 %	(h)
Thessaloniki, Greece	40.63° N/22.95° E	1993–1996	−4.0 %	(e)
Thessaloniki, Greece	idem	1990–1998	−4.5 %	(a)

ACPD
14, 16529–16589, 2014

Table 8. Absolute and relative trends of AOD at different stations from (a): Alpert et al. (2012), (b): Nyeki et al. (2012), (c): Fitzka et al. (2012), (d): Kazadzis et al. (2007).

Station, Country	Latitude/Longitude	Period	Trend/decade	Reference
Berlin[a], Germany	52.50° N/13.40° E	2002–2010	−20.5 %	(a)
Berlin[b], Germany	idem	2002–2010	−17.9 %	(a)
Berlin[c], Germany	idem	2002–2010	−12.3 %	(a)
Warsaw[a], Poland	52.30° N/21.00° E	2002–2010	−2.4 %	(a)
Warsaw[b], Poland	idem	2002–2010	−0.4 %	(a)
Warsaw[c], Poland	idem	2002–2010	+12.9 %	(a)
Ruhr Area[a], Germany	51.50° N/7.50° E	2002–2010	−15.7 %	(a)
Ruhr Area[b], Germany	idem	2002–2010	−9.3 %	(a)
Ruhr Area[c], Germany	idem	2002–2010	−9.3 %	(a)
Paris[a], France	48.90° N/2.40° E	2002–2010	−8.1 %	(a)
Paris[b], France	idem	2002–2010	+5.0 %	(a)
Paris[c], France	idem	2002–2010	+9.8 %	(a)
Hohenpeisenberg, Germany	47.80° N/11.00° E	1995–2010	−10.6 %	(b)
Hoher Sonnblick, Austria	47.05° N/12.96° E	1997–2011	−5 to −6 %	(c)
Barcelona[a], Spain	41.40° N/2.20° E	2002–2010	−8.8 %	(a)
Barcelona[b], Spain	idem	2002–2010	+4.2 %	(a)
Barcelona[c], Spain	idem	2002–2010	−2.3 %	(a)
Thessaloniki, Greece	40.63° N/22.95° E	1997–2006	−29.0 %	(d)
Madrid[a], Spain	40.40° N/3.70° W	2002–2010	−18.3 %	(a)
Madrid[b], Spain	idem	2002–2010	−10.0 %	(a)
Madrid[c], Spain	idem	2002–2010	−7.4 %	(a)

MODIS-Terra, MODIS-Aqua and MISR measurements are represented by respectively a "[a]", "[b]" and "[c]" after the station name.

ACPD
14, 16529–16589, 2014

Table 9. Performance of the seasonal regression models.

	Spring	Summer	Autumn	Winter
Correlation	0.95	0.93	0.97	0.90
Regression equation	$y = 0.89x + 145.17$	$y = 0.94x + 104.36$	$y = 0.90x + 102.48$	$y = 0.91x + 8.13$
MBE	−4 %	−2 %	0.06 %	−7 %
MABE	14 %	6 %	15 %	15 %

ACPD
14, 16529–16589, 2014

Table 10. Seasonal changes in UV caused by changes in S_g, Q_{O_3} and τ_{aer}.

	Spring	Summer	Autumn	Winter
τ_{aer}	1 %	−1 %	2 %	4 %
Q_{O_3}	−9 %	−4 %	−2 %	−15 %
S_g	37 %	18 %	53 %	32 %

ACPD
14, 16529–16589, 2014

Table 11. Results of MLR analysis with only S_g, S_g combined with Q_{O_3} and S_g combined with τ_{aer} as explanatory variables.

	S_g	$S_g + Q_{O_3}$	$S_g + \tau_{aer}$
Adjusted R^2			
Spring	0.85	0.90	0.85
Summer	0.81	0.85	0.81
Autumn	0.95	0.95	0.95
Winter	0.65	0.81	0.65
MABE (in %)			
Spring	14.53	14.40	14.33
Summer	6.39	6.21	6.21
Autumn	15.45	15.25	14.89
Winter	22.20	14.25	21.47
Correlation modeled and measured UV values			
Spring	0.93	0.95	0.93
Summer	0.91	0.93	0.91
Autumn	0.96	0.96	0.96
Winter	0.75	0.89	0.76

ACPD
14, 16529–16589, 2014

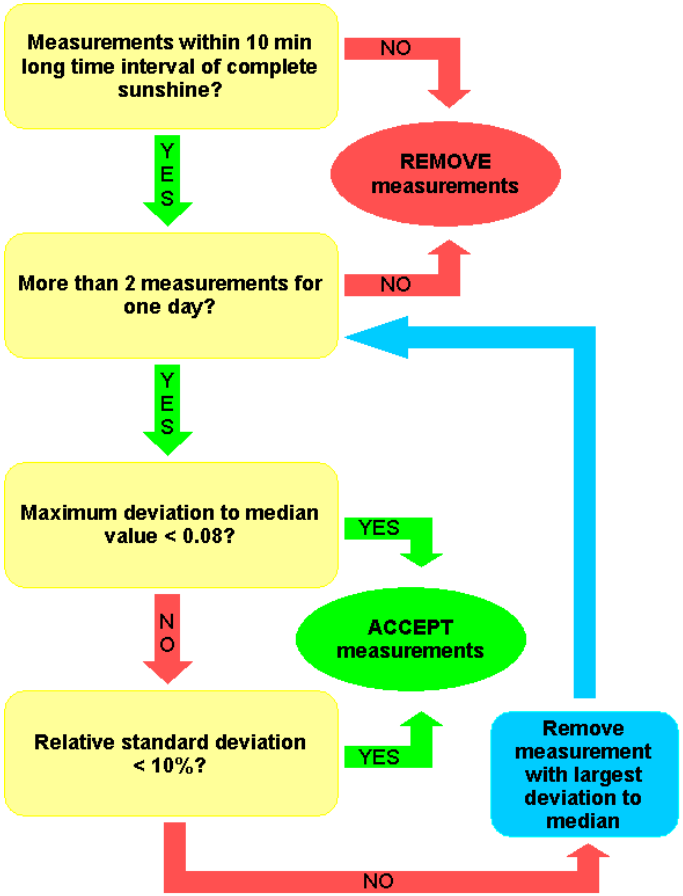

Figure 1. Improved cloud screening procedure.

ACPD
14, 16529–16589, 2014

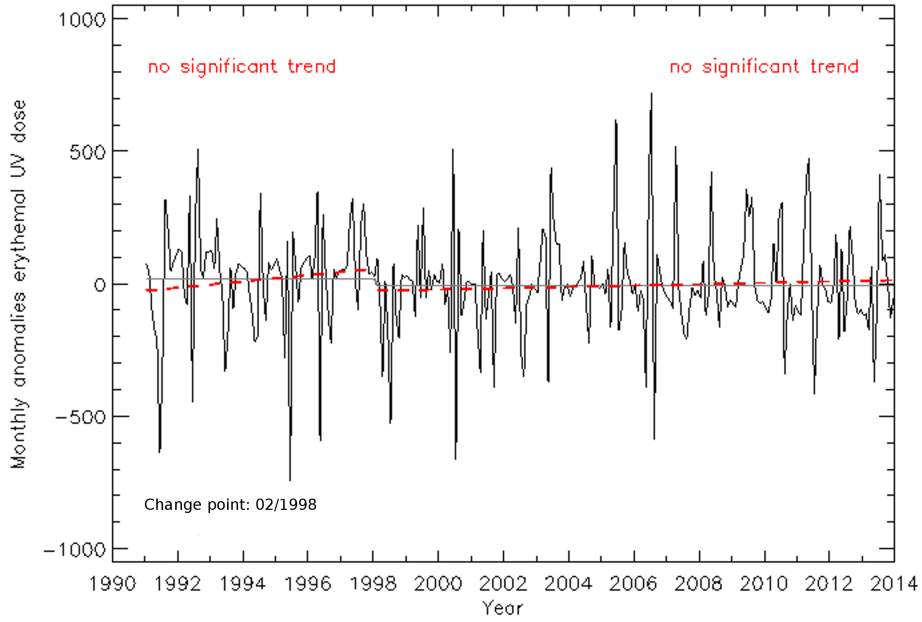

Figure 2. The black line represents the detrended time series of monthly anomalies of erythemal UV dose (1991–2013). The red (dashed) lines represent the (insignificant) positive trends before and after the detected change point. The grey lines represent the mean before and after the change point.

ACPD
14, 16529–16589, 2014

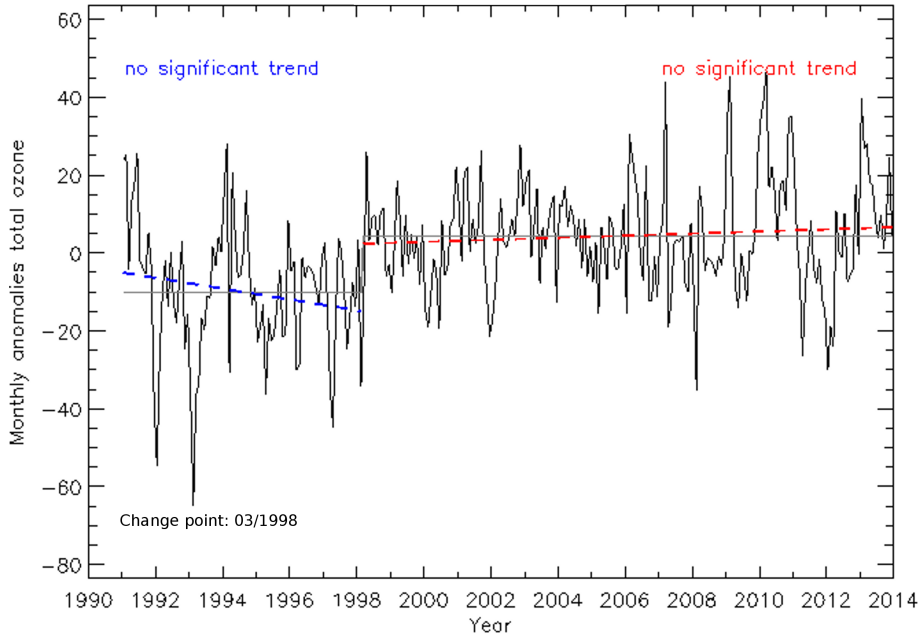

Figure 3. The black line represents the time series of monthly anomalies of total ozone column (1991–2013). The blue (dashed) line represents the (insignificant) negative trend before the detected change point and the red (dashed) line represents the (insignificant) positive trend after the change point. The grey lines represent the mean before and after the change point.

ACPD
14, 16529–16589, 2014

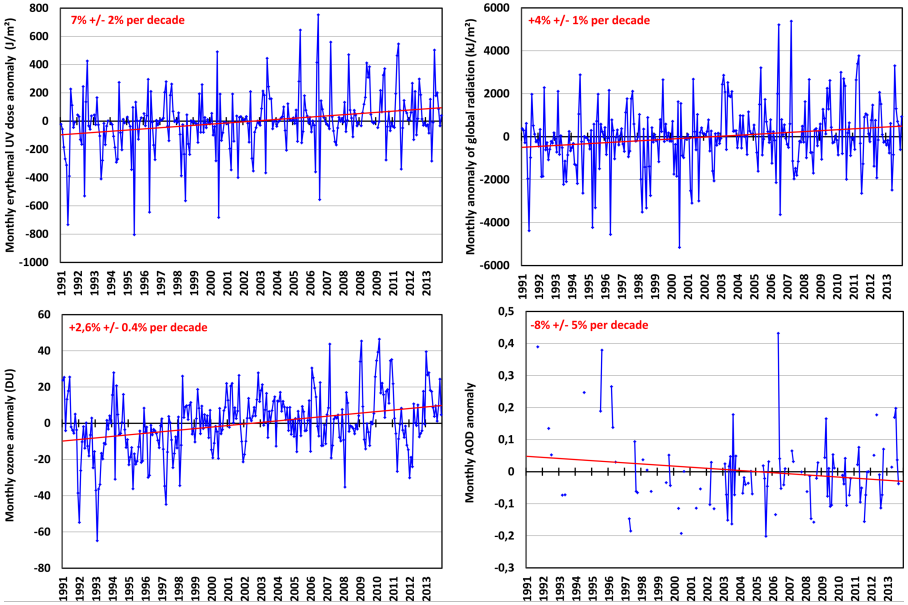

Figure 4. Trends of monthly anomalies at Uccle for erythemal UV dose (upper left panel, global solar radiation (upper right panel), total ozone column (lower left panel) and AOD at 320.1 nm (lower right panel) for the time period 1991–2013. The blue lines represent the time series, whereas the red lines represent the trend over the time period.

ACPD
14, 16529–16589, 2014

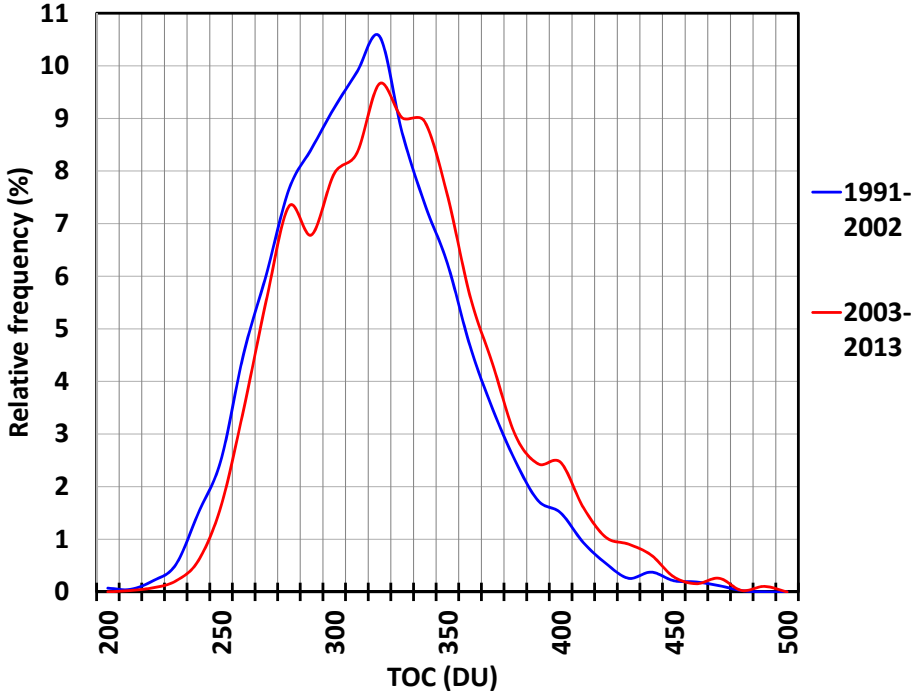

Figure 5. Relative frequency distribution of daily TOC values for the two time periods: 1991–2002 (in blue) and 2003–2013 (in red).

ACPD
14, 16529–16589, 2014

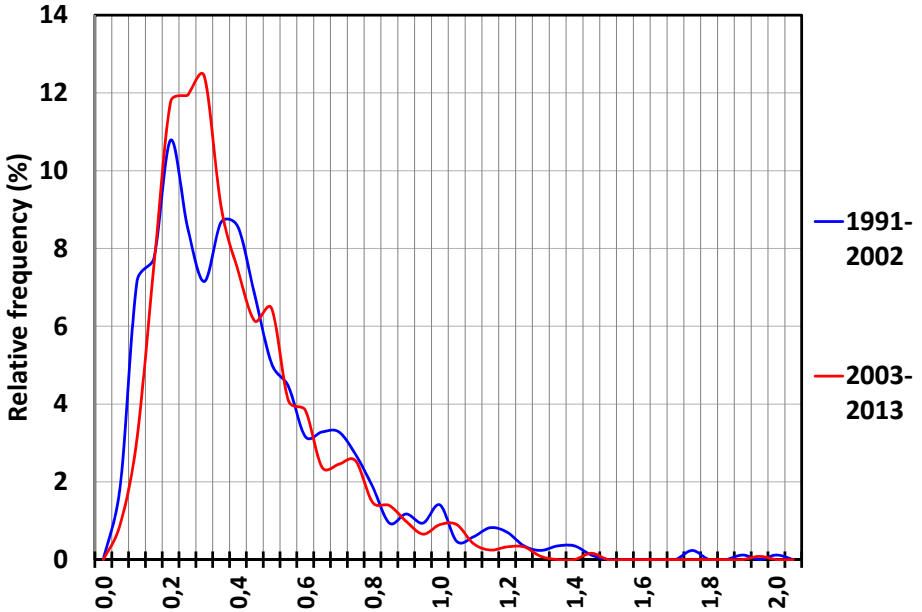

Figure 6. Relative frequency distribution of daily AOD values for the two time periods: 1991–2002 (in blue) and 2003–2013 (in red).

ACPD
14, 16529–16589, 2014

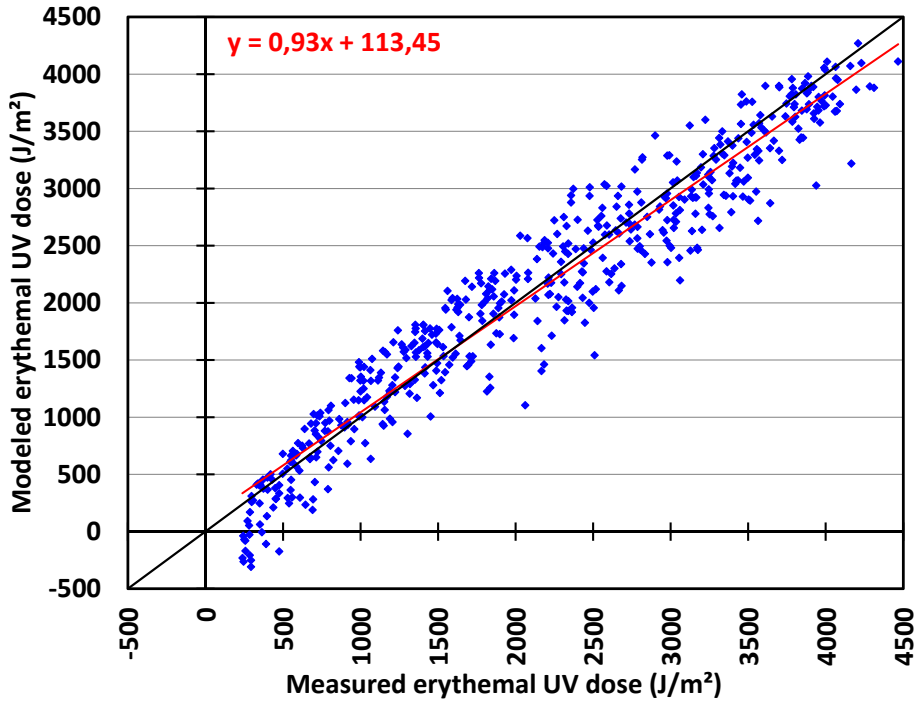

Figure 7. Scatterplot of the measured and modeled erythemal UV doses at Uccle for the 2009–2013 validation period. The red line represents the regression line of the data ($f(x) = 0.93x + 113.45$). The black line is the $f(x) = x$ line.

ACPD
14, 16529–16589, 2014

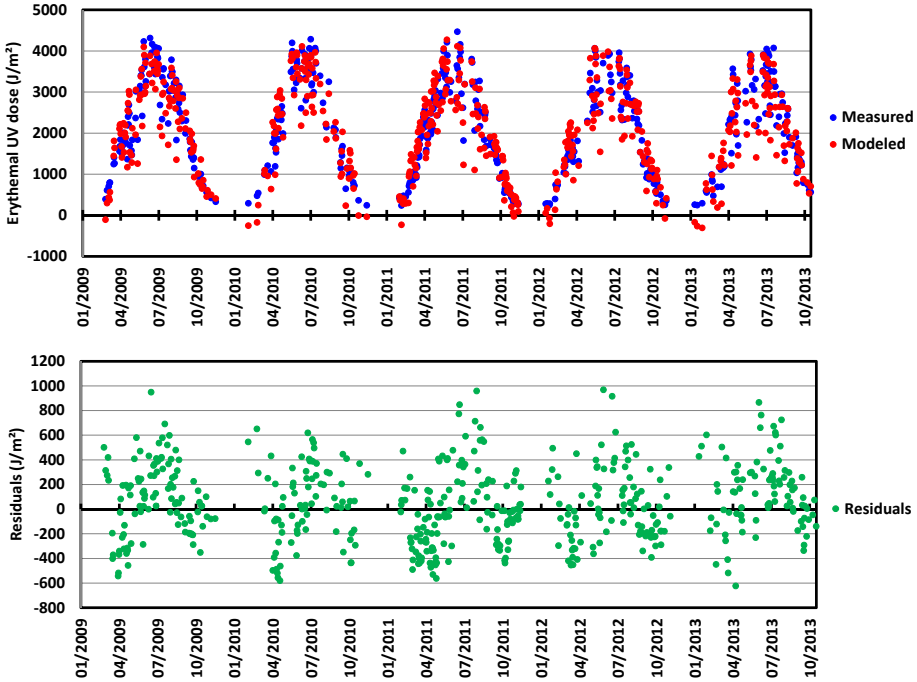

Figure 8. Validation of the multiple linear regression equation: the upper panel shows the measured (in blue) and modeled (in red) erythemal UV values; the lower panel presents the absolute residuals.

ACPD
14, 16529–16589, 2014

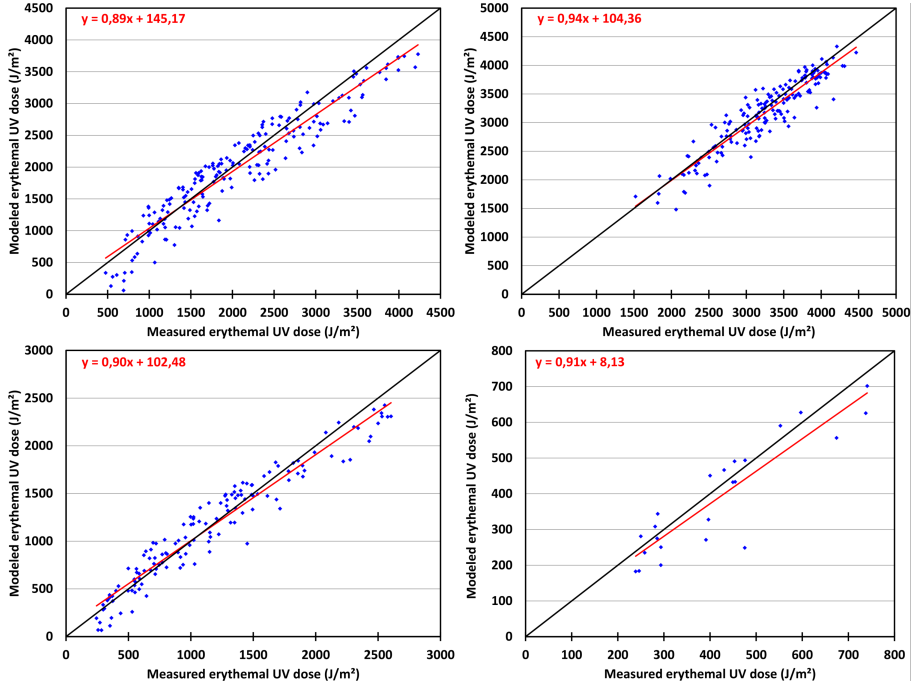

Figure 9. Scatterplots of the measured and modeled erythemal UV doses at Uccle for the 2009–2013 validation period for spring (upper left panel), summer (upper right panel), autumn (lower left panel) and winter (lower right panel). The red lines represent the regression lines of the data and the black lines are the $f(x) = x$ lines.

ACPD
14, 16529–16589, 2014

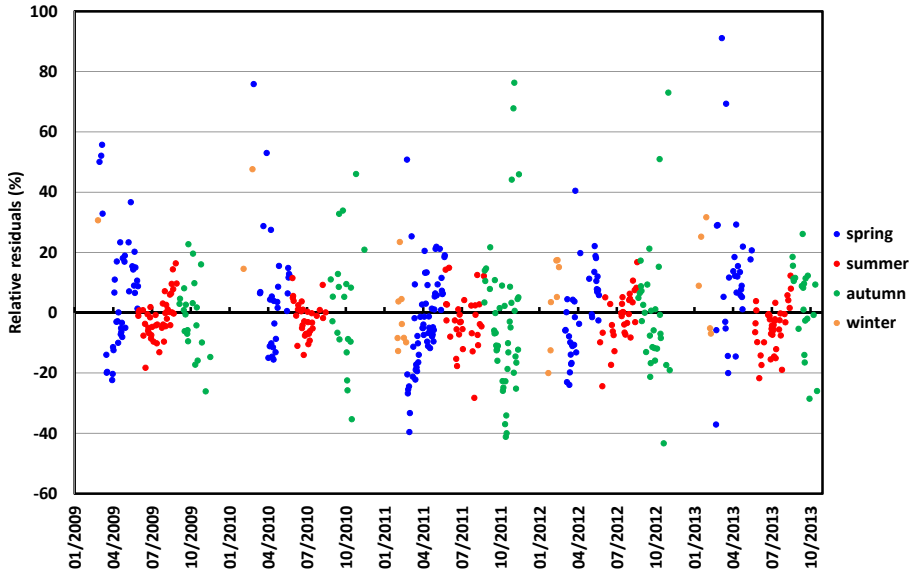

Figure 10. Relative residuals (= (measured – modeled)/measured × 100) of the seasonal multiple regression models. The colors represent the different seasons: blue=spring; red=summer; green=autumn; orange=winter.

ACPD
14, 16529–16589, 2014